Chapter 4

Free-Space Propagation of Gaussian-Beam Waves

Overview: The purpose of this chapter is to introduce the basic features of a *Gaussian-beam wave* in both the plane of the transmitter and the plane of the receiver. Our main concentration of study involves the lowest-order mode or TEM_{00} beam, but we also briefly introduce *Hermite-Gaussian* and *Laguerre-Gaussian beams* as higher-order modes, or additional solutions, of the *paraxial wave equation.* Each of these higher-order modes produces a pattern of multiple spots in the receiver plane as opposed to a single (circular) spot from a lowest-order beam wave. Consequently, the analysis of such beams is more complex than that of the TEM_{00} beam. One advantage in working with the TEM_{00} Gaussian-beam wave model is that it also includes the limiting classical cases of an infinite *plane wave* and a *spherical wave.*

We facilitate the free-space analysis of Gaussian-beam waves by introducing two sets of *nondimensional beam parameters*—one set that characterizes the beam in the plane of the transmitter and another set that does the same in the plane of the receiver. The beam *spot radius* and *phase front radius of curvature*, as well as other beam properties, are readily determined from either set of beam parameters. For example, we use the beam parameters to identify the size and location of the *beam waist* and the *geometric focus.* The consistent use of these beam parameters in all the remaining chapters of the text facilitates the analysis of Gaussian-beam waves propagating through random media.

When optical elements such as aperture stops and lenses exist at various locations along the propagation path, the method of *ABCD ray matrices* can be used to characterize these elements (including the free-space propagation between elements). By cascading the matrices in sequence, the entire optical path between the input and output planes can be represented by a single 2×2 matrix. The use of these ray matrices, which is based on the paraxial approximation, greatly simplifies the treatment of propagation through several such optical elements. In later chapters we will extend this technique to propagation paths that also include atmospheric turbulence along portions of the path.

4.1 Introduction

The mathematical description of a propagating wave involves the notion of a field. Basically, a *field* $u(\mathbf{R}, t)$ is a function of space $\mathbf{R} = (x, y, z)$ and time t that satisfies a partial differential equation. In the case of electromagnetic radiation, the field may be a transverse electromagnetic (TEM) wave, whereas for acoustic waves the field may represent a pressure wave. The governing equation in most cases is the *wave equation*

$$\nabla^2 u = \frac{1}{c^2}\frac{\partial^2 u}{\partial t^2}, \tag{1}$$

where c represents the speed of the propagating wave and ∇^2 is the Laplacian operator defined in rectangular coordinates by

$$\nabla^2 u = \frac{\partial^2 u}{\partial x^2} + \frac{\partial^2 u}{\partial y^2} + \frac{\partial^2 u}{\partial z^2}. \tag{2}$$

For electromagnetic waves, the constant $c = 3 \times 10^8$ m/s is the *speed of light.*

If we assume that time variations in the field are sinusoidal (i.e., a *monochromatic wave*), then we look for solutions of (1) of the form $u(\mathbf{R}, t) = U_0(\mathbf{R})e^{-i\omega t}$, where ω is the *angular frequency* and $U_0(\mathbf{R})$ is the *complex amplitude* of the wave.[1] The substitution of this solution form into Eq. (1) leads to the time-independent *reduced wave equation* (or *Helmholtz equation*)

$$\nabla^2 U_0 + k^2 U_0 = 0, \tag{3}$$

where k is the optical wave number related to the optical wavelength λ by $k = \omega/c = 2\pi/\lambda$.

4.2 Paraxial Wave Equation

For optical wave propagation, we can further reduce the Helmholtz equation (3) to what is called the paraxial wave equation. To begin, let us assume the beam originates in the plane at $z = 0$ and propagates along the positive z-axis. If we also assume the free-space optical field at any point along the propagation path remains rotationally symmetric, then it can be expressed as a function of $r = \sqrt{x^2 + y^2}$ and z. Thus, the reduced wave equation (3) in cylindrical coordinates can be written as

$$\frac{1}{r}\frac{\partial}{\partial r}\left(r\frac{\partial U_0}{\partial r}\right) + \frac{\partial^2 U_0}{\partial z^2} + k^2 U_0 = 0. \tag{4}$$

For reasons of simplification in the solution process, it is customary to first make the substitution $U_0(r, z) = V(r, z)e^{ikz}$ in Eq. (4), which leads to

$$\frac{1}{r}\frac{\partial}{\partial r}\left(r\frac{\partial V}{\partial r}\right) + \frac{\partial^2 V}{\partial z^2} + 2ik\frac{\partial V}{\partial z} = 0. \tag{5}$$

To further simplify Eq. (5), we make use of the so-called "paraxial approximation."

4.2.1 Paraxial approximation

The paraxial approximation is based on the notion that the propagation distance for an optical wave along the z-axis is much greater than the transverse spreading of the wave. Thus, if $\mathbf{R} = (\mathbf{r}, z)$ and $\mathbf{S} = (\mathbf{s}, 0)$ denote two points in space with $\mathbf{r}$ and $\mathbf{s}$

[1] Because the time factor $e^{-i\omega t}$ of the field is usually omitted in wave propagation studies, it is common practice to also refer to the complex amplitude $U_0(\mathbf{R})$ as the (spatial) field.

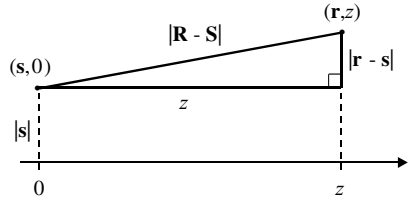

Figure 4.1 Geometry for Eq. (6).

transverse to the propagation axis, then the distance between such points is (see Fig. 4.1)

$$|\mathbf{R}-\mathbf{S}| = \left(z^2+|\mathbf{r}-\mathbf{s}|^2\right)^{1/2} = z\left(1+\frac{|\mathbf{r}-\mathbf{s}|^2}{z^2}\right)^{1/2}. \tag{6}$$

If we assume that the transverse distance is much smaller than the longitudinal propagation distance between the points, then we may expand the second factor in (6) in a binomial series to obtain

$$\begin{aligned}|\mathbf{R}-\mathbf{S}| &= z\left(1+\frac{|\mathbf{r}-\mathbf{s}|^2}{2z^2}+\cdots\right)\\ &= z+\frac{|\mathbf{r}-\mathbf{s}|^2}{2z}+\cdots, \quad |\mathbf{r}-\mathbf{s}| \ll z.\end{aligned} \tag{7}$$

Dropping all remaining terms on the right-hand side of Eq. (7) after the first two shown constitutes what is called the *paraxial approximation.*

As a consequence of the paraxial assumption leading to (7), it follows that

$$\left|\frac{\partial^2 V}{\partial z^2}\right| \ll \left|2k\frac{\partial V}{\partial z}\right|, \quad \left|\frac{\partial^2 V}{\partial z^2}\right| \ll \left|\frac{1}{r}\frac{\partial}{\partial r}\left(r\frac{\partial V}{\partial r}\right)\right|. \tag{8}$$

The inequalities (8) are based on the fact that diffraction effects on the optical wave $V(r, z)$ change slowly with respect to propagation distance z, and also with respect to transverse variations due to the finite size of the beam. The significance of these inequalities is that they permit us to set $\partial^2 V/\partial z^2 = 0$ in Eq. (5), from which we obtain the *paraxial wave equation*[2]

$$\frac{1}{r}\frac{\partial}{\partial r}\left(r\frac{\partial V}{\partial r}\right)+2ik\frac{\partial V}{\partial z}=0. \tag{9}$$

There are basically two methods of solution of (9), one called the *direct method* and the other relying on the *Huygens-Fresnel integral* (see Sections 4.3.3 and 4.3.4).

[2]Equation (9) is also known as the *parabolic equation.*

4.3 Optical Wave Models

Most theoretical treatments of optical wave propagation have concentrated on simple field models such as an unbounded plane wave or spherical wave, the latter often taken as a point source. However, in many applications the plane wave and spherical wave approximations are not sufficient to characterize propagation properties of the wave, particularly when focusing and diverging characteristics are important. In such cases the lowest-order Gaussian-beam wave model is usually introduced, limiting forms of which lead to the plane wave and spherical wave models. For certain types of lasers it may also be necessary to introduce the higher-order Gaussian modes in either rectangular or cylindrical coordinates (e.g., see Section 4.7 and also Chap. 17).

4.3.1 Plane wave and spherical wave models

A *plane wave* is defined as one in which the equiphase surfaces (phase fronts) form parallel planes. The mathematical description of a general plane wave in the plane of the transmitter at $z = 0$ is

$$z = 0: \qquad U_0(r, 0) = A_0 e^{i\varphi_0}, \tag{10}$$

where A_0 is a constant that represents the strength or *amplitude* of the wave field and φ_0 is the *phase*. If the plane wave is propagating along the positive z-axis in free space, the complex amplitude at distance z from the transmitter takes the form [1,2]

$$z > 0: \qquad U_0(r, z) = V(r, z)e^{ikz} = A_0 e^{i\varphi_0 + ikz}, \tag{11}$$

where $V(r, z) = A_0 e^{i\varphi_0}$ represents a solution of the paraxial wave equation (9). Hence, the plane wave field remains that of a plane wave with changes occurring only in the phase.

A *spherical wave* is characterized by concentric spheres forming the equiphase surfaces. For a spherical wave emanating from the origin, we have

$$z = 0: \qquad U_0(r, 0) = \lim_{R \to 0} \frac{A_0 e^{ikR}}{4\pi R} \cong A_0 \delta(\mathbf{r}), \tag{12}$$

where $\delta(\mathbf{r})$ is the *Dirac delta function.* At distance z from the transmitter, the solution of the paraxial wave equation for an initial spherical wave leads to [2]

$$z > 0: \quad U_0(r, z) = \frac{A_0}{4\pi z} \exp\left(ikz + \frac{ikr^2}{2z} \right) = A \exp\left[ik\left(z + \frac{r^2}{2z} \right) \right]. \tag{13}$$

Here the amplitude $A = A_0/4\pi z$ is scaled by distance and the phase $\varphi = k(z + r^2/2z)$ has a transverse radial dependency. Because (13) represents the solution of (9) for a point source input (12), it also represents a form of *free-space Green's function* for the paraxial wave equation (see Section 4.3.4).

4.3.2 Lowest-order Gaussian-beam wave

Let us consider the propagation in free space of a lowest-order transverse electromagnetic (TEM) *Gaussian-beam wave*, also called a TEM_{00} wave. It is assumed the transmitting aperture is located in the plane $z = 0$ and the amplitude distribution in this plane is Gaussian with effective beam radius (spot size) W_0 [m], where W_0 denotes the radius at which the field amplitude falls to $1/e$ of that on the beam axis as shown in Fig. 4.2. In addition, the phase front is taken to be parabolic with radius of curvature F_0 [m]. The particular cases $F_0 = \infty, F_0 > 0$, and $F_0 < 0$ correspond to *collimated, convergent*, and *divergent* beam forms, respectively (see Fig. 4.3). If the field of the wave at $z = 0$ has amplitude a_0 $[(W/\text{m}^2)^{1/2}]$ on the optical axis ($r = 0$), it is therefore described by [2]

$$z = 0: \quad U_0(r, 0) = a_0 \exp\left(-\frac{r^2}{W_0^2} - \frac{ikr^2}{2F_0}\right) = a_0 \exp\left(-\frac{1}{2}\alpha_0 k r^2\right), \tag{14}$$

where $r = \sqrt{x^2 + y^2}$ is radial distance from the beam center line and α_0 is a complex parameter related to spot size and phase front radius of curvature according to

$$\alpha_0 = \frac{2}{kW_0^2} + i\frac{1}{F_0}. \quad [\text{m}^{-1}] \tag{15}$$

In comparing the functional form (14) with that of an unbounded plane wave [see Eq. (10)], we identify the *amplitude* and *phase*, respectively, of a Gaussian-beam wave as

$$A_0 = a_0 \exp\left(-\frac{r^2}{W_0^2}\right), \tag{16}$$

$$\varphi_0 = -\frac{kr^2}{2F_0}. \tag{17}$$

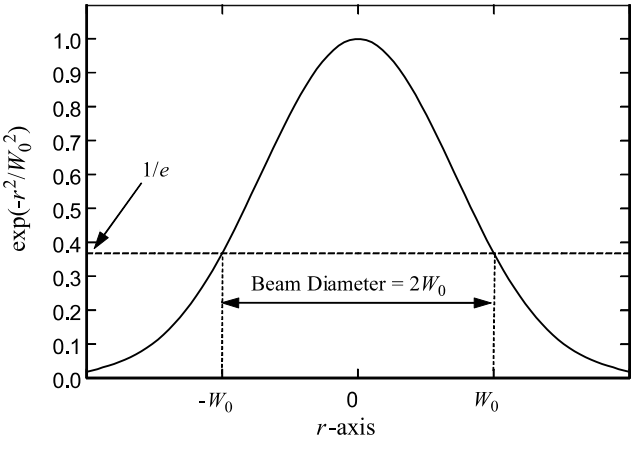

Figure 4.2 Amplitude profile of a Gaussian-beam wave.

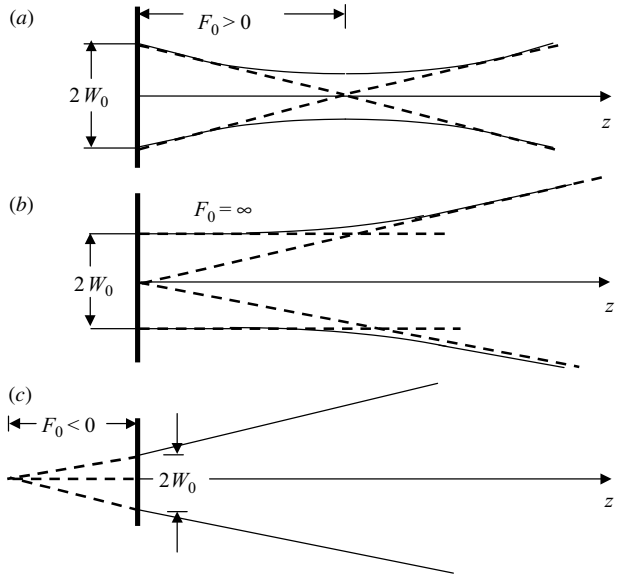

Figure 4.3 (*a*) Convergent beam, (*b*) collimated beam, and (*c*) divergent beam.

Thus, both amplitude and phase of a Gaussian-beam wave depend on the transverse distance r. The negative sign appearing in the phase (17) is a consequence of the sign convention used to define the phase front radius of curvature F_0.

4.3.3 Paraxial equation: direct solution method

To directly solve the paraxial wave equation (9), we will explicitly look for a Gaussian function as a solution. Hence, we start by looking for solutions of the general form [3,4]

$$V(r,z) = A(z)\exp\left[-\frac{1}{p(z)}\left(\frac{\alpha_0 k r^2}{2}\right)\right], \tag{18}$$

where $A(z)$ represents the on-axis complex amplitude of the wave and $p(z)$ is a propagation parameter related to the complex radius of curvature. Clearly, in order that Eq. (18) reduce to the initial Gaussian-beam form given by Eq. (14), these functions must satisfy the *initial conditions*

$$\begin{aligned} p(0) &= 1, \\ A(0) &= a_0 = 1, \end{aligned} \tag{19}$$

where we now set $a_0 = 1$ for mathematical convenience. By substituting Eq. (18) into (9) and simplifying, we obtain

$$\alpha_0^2 k^2 r^2 A(z) + i\alpha_0 k^2 r^2 A(z)p'(z) - 2\alpha_0 k A(z)p(z) + 2ikA'(z)p^2(z) = 0. \tag{20}$$

Next, by setting terms involving like powers of r to zero, we obtain the pair of simple first-order differential equations

$$r^2\text{:} \quad p'(z) = i\alpha_0 = -\frac{1}{F_0} + i\frac{2}{kW_0^2}, \tag{21}$$

$$r^0\text{:} \quad A'(z) = -\frac{i\alpha_0}{p(z)}A(z) = -\frac{p'(z)}{p(z)}A(z). \tag{22}$$

The simultaneous solution of Eqs. (21) and (22) together with the initial conditions (19) yield

$$\begin{aligned} p(z) &= 1 + i\alpha_0 z = 1 - \frac{z}{F_0} + i\frac{2z}{kW_0^2}, \\ A(z) &= \frac{1}{p(z)} = \frac{1}{1 + i\alpha_0 z}. \end{aligned} \tag{23}$$

In summary, the complex amplitude at distance z from the source is the Gaussian-beam wave

$$\begin{aligned} U_0(r,z) = V(r,z)e^{ikz} &= \frac{1}{1+i\alpha_0 z}\exp\left[ikz - \frac{1}{2}\left(\frac{\alpha_0 k}{1+i\alpha_0 z}\right)r^2\right] \\ &= \frac{1}{1+i\alpha_0 z}\exp\left[ikz + \frac{ik}{2z}\left(\frac{i\alpha_0 z}{1+i\alpha_0 z}\right)r^2\right], \end{aligned} \tag{24}$$

where the final form of (24) is chosen for later mathematical convenience.

4.3.4 Paraxial equation: Huygens-Fresnel integral

The Huygens-Fresnel integral provides another method of analysis that leads to the same result as Eq. (24) for the complex amplitude at position z along the propagation path, but has the distinct advantage that it can be extended to the case where the propagation path includes several optical elements arbitrarily distributed along the path (e.g., see Sections 4.9 and 4.10). In the present formulation, the complex amplitude at propagation distance z from the source is represented by the *Huygens-Fresnel integral* [4,5]

$$U_0(\mathbf{r},z) = -2ik\int\int_{-\infty}^{\infty} G(\mathbf{s},\mathbf{r};z)U_0(\mathbf{s},0)d^2s, \tag{25}$$

where $U_0(\mathbf{s},0)$ is the optical wave at the source plane and $G(\mathbf{s},\mathbf{r};z)$ is the *free-space Green's function.* In general, the free-space Green's function is a spherical wave which, under the paraxial approximation, can be expressed as [recall Eqs. (7) and (13)]

$$G(\mathbf{s},\mathbf{r};z) = \frac{e^{ik|\mathbf{R}-\mathbf{S}|}}{4\pi|\mathbf{R}-\mathbf{S}|} \cong \frac{1}{4\pi z}\exp\left[ikz + \frac{ik}{2z}|\mathbf{s}-\mathbf{r}|^2\right]. \tag{26}$$

Although we will not do so here (see Example 4 in Worked Examples), it can be shown that Eq. (25) represents a formal solution of the initial value problem

$$\begin{aligned} &\frac{1}{r}\frac{\partial}{\partial r}\left(r\frac{\partial V}{\partial r}\right)+2ik\frac{\partial V}{\partial z}=0,\\ &V(r,0)\equiv U_0(r,0)=\exp\left(-\frac{r^2}{W_0^2}-\frac{ikr^2}{2F_0}\right), \end{aligned} \tag{27}$$

where $V(r,z)=U_0(r,z)e^{-ikz}$. Instead, we illustrate that the optical wave represented by Eq. (25) is the same as that given by Eq. (24). We start by writing the complex amplitude of the Gaussian-beam wave at the source plane $z=0$ as

$$U_0(\mathbf{s},0)=\exp\left(-\frac{1}{2}\alpha_0 ks^2\right)=\exp\left[\frac{ik}{2z}(i\alpha_0 z)s^2\right]. \tag{28}$$

The substitution of Eq. (28) into Eq. (25) yields

$$\begin{aligned} U_0(\mathbf{r},z)&=-\frac{ik}{2\pi z}\exp\left(ikz+\frac{ik}{2z}r^2\right)\int\int_{-\infty}^{\infty}\exp\left(-\frac{ik}{z}\mathbf{r}\cdot\mathbf{s}\right)\exp\left[\frac{ik}{2z}(1+i\alpha_0 z)s^2\right]d^2s\\ &=-\frac{ik}{2\pi z}\exp\left(ikz+\frac{ik}{2z}r^2\right)\int_0^{\infty}\int_0^{2\pi}\exp\left(-\frac{ik}{z}rs\cos\theta\right)\\ &\quad\times\exp\left[\frac{ik}{2z}(1+i\alpha_0 z)s^2\right]s\,d\theta\,ds, \end{aligned} \tag{29}$$

where we have changed to polar coordinates in the second step, i.e., $d^2s=s\,d\theta\,ds$. Performing the inside integration yields (integral #9 in Appendix II)

$$\int_0^{2\pi}\exp\left(-\frac{ik}{z}rs\cos\theta\right)d\theta=2\pi J_0\left(\frac{krs}{z}\right), \tag{30}$$

where $J_0(x)$ is a Bessel function of the first kind and order zero [6]. The remaining integration on s gives us (integral #10 in Appendix II)

$$\begin{aligned} U_0(r,z)&=-\frac{ik}{z}\exp\left(ikz+\frac{ik}{2z}r^2\right)\int_0^{\infty}sJ_0\left(\frac{krs}{z}\right)\exp\left[\frac{ik}{2z}(1+i\alpha_0 z)s^2\right]ds\\ &=\frac{1}{1+i\alpha_0 z}\exp\left[ikz+\frac{ik}{2z}\left(\frac{i\alpha_0 z}{1+i\alpha_0 z}\right)r^2\right], \end{aligned} \tag{31}$$

which is the same as Eq. (24). Thus, we have established the equivalence of the direct method and the Huygens-Fresnel integral.

4.4 Diffractive Properties of Gaussian-Beam Waves

Early studies of the diffractive characteristics of Gaussian-beam waves for the design and analysis of laser systems include those of Refs. [3,7–12]. Kogelnik and Li [3] provide a good review of the basic theory of laser beams and resonators,

and they also discuss the use of *ABCD* ray matrices to illustrate Gaussian-beam wave propagation through optical structures. Graphical representations of Gaussian-beam wave propagation in optical resonators with circle diagrams were first proposed by Collins [8], and Li [9] extended the notion to the case of dual circles. Arnaud [13] suggested a graphic method for determining the beam parameters that is essentially the $y\bar{y}$ diagram method introduced by Delano [7]. Kessler and Schack [14] illustrated the utility of the $y\bar{y}$ diagram method as a helpful design tool for synthesizing and analyzing optical systems. Andrews et al. [15] developed a method of Gaussian-beam wave analysis through the use of two pairs of Gaussian-beam parameters that are linked through an elementary conformal transformation. The basic beam characteristics are readily identified in either plane through simple geometric and analytic relations. In this chapter we review the basic notation and relations introduced in Ref. [15], which in turn are utilized in our subsequent analysis of Gaussian-beam wave propagation through random media. We believe the consistent use of these beam parameters throughout the text can assist the development of physical intuition for the reader.

4.4.1 Input plane beam parameters

Let us consider the line-of-sight propagation of a Gaussian beam from the input plane positioned at $z = 0$ to the output plane at $z > 0$. By *line of sight*, we mean the transmitter and receiver are able to "see" each other (no optical elements exist between input and output planes). To begin, we express the propagation parameter $p(z)$ in the form [see Eqs. (23)]

$$p(z) = 1 + i\alpha_0 z = \Theta_0 + i\Lambda_0, \tag{32}$$

where Θ_0 and Λ_0 are the real and imaginary parts of $p(z)$ defined by

$$\Theta_0 = 1 - \frac{z}{F_0}, \quad \Lambda_0 = \frac{2z}{kW_0^2}. \tag{33}$$

Next, by making the observation

$$\begin{aligned} \frac{i\alpha_0 z}{1 + i\alpha_0 z} &= 1 - \frac{1}{\Theta_0 + i\Lambda_0} \\ &= \frac{\Theta_0(\Theta_0 - 1) + \Lambda_0^2}{\Theta_0^2 + \Lambda_0^2} + i\frac{\Lambda_0}{\Theta_0^2 + \Lambda_0^2} \end{aligned}$$

and writing

$$p(z) = \sqrt{\Theta_0^2 + \Lambda_0^2}\exp\left(i\tan^{-1}\frac{\Lambda_0}{\Theta_0}\right), \tag{34}$$

it follows from Eq. (24) that

$$U_0(r,z) = \frac{1}{1+i\alpha_0 z}\exp\left[ikz + \frac{ik}{2z}\left(\frac{i\alpha_0 z}{1+i\alpha_0 z}\right)r^2\right] = \frac{1}{\sqrt{\Theta_0^2+\Lambda_0^2}}\exp\left(-\frac{r^2}{W^2}\right)\exp\left[i\left(kz-\varphi-\frac{kr^2}{2F}\right)\right], \tag{35}$$

where φ, W, and F represent the *longitudinal phase shift, spot size radius*, and *radius of curvature* at position z along the propagation path. These quantities are defined, respectively, in terms of beam parameters Θ_0 and Λ_0 by

$$\varphi = \tan^{-1}\frac{\Lambda_0}{\Theta_0}, \tag{36}$$

$$W = W_0\sqrt{\Theta_0^2+\Lambda_0^2}, \tag{37}$$

$$F = \frac{kW_0^2}{2}\left[\frac{\Lambda_0\left(\Theta_0^2+\Lambda_0^2\right)}{\Theta_0(1-\Theta_0)-\Lambda_0^2}\right] = \frac{F_0\left(\Theta_0^2+\Lambda_0^2\right)(\Theta_0-1)}{\Theta_0^2+\Lambda_0^2-\Theta_0}. \tag{38}$$

Because they involve beam characteristics at the input plane (transmitter), we refer to the pair of nondimensional quantities Θ_0 and Λ_0 as *input plane* (or *transmitter*) *beam parameters.* The parameter Θ_0 is also called the *curvature parameter* and Λ_0 is the *Fresnel ratio* at the input plane. For fixed path length $z = L$ and radius of curvature F_0, the curvature parameter identifies collimated, convergent, and divergent beam forms, respectively, according to $\Theta_0 = 1$, $\Theta_0 < 1$, and $\Theta_0 > 1$.

By examination of Eq. (35), we recognize that the input plane beam parameters Θ_0 and Λ_0 characterize the refractive (focusing) and diffractive changes, respectively, in the on-axis amplitude of the Gaussian beam. In particular, after propagating a distance z, the on-axis amplitude of the beam takes the form

$$A = \frac{1}{\sqrt{\underbrace{(1-z/F_0)^2}_{\textbf{refraction}}+\underbrace{(2z/kW_0^2)^2}_{\textbf{diffraction}}}} = \frac{1}{\sqrt{\Theta_0^2+\Lambda_0^2}}. \tag{39}$$

For a Gaussian-beam wave, the longitudinal phase shift (36) varies from zero at the transmitter up to π as the propagation path length becomes infinite (see Section 4.5). In the limiting case of a plane wave, however, this phase shift is always zero because $\Lambda_0 = 0$. Except for a convergent beam, diffraction effects cause the spot size radius of the beam (37) to increase steadily along the entire propagation path. That is, the spot radius will initially decrease for a transmitted convergent beam until it reaches the waist region and then increase in accordance with the spot radius of a collimated beam [see Fig. 4.3(*a*)]. To illustrate the general behavior of the phase front radius of curvature (38) along the propagation path, we plot the ratio F/F_0 as a function of scaled distance z/F_0 in Fig. 4.4 for a convergent beam in which $2F_0/kW_0^2 = 1$. Observe that the radius of curvature has a positive

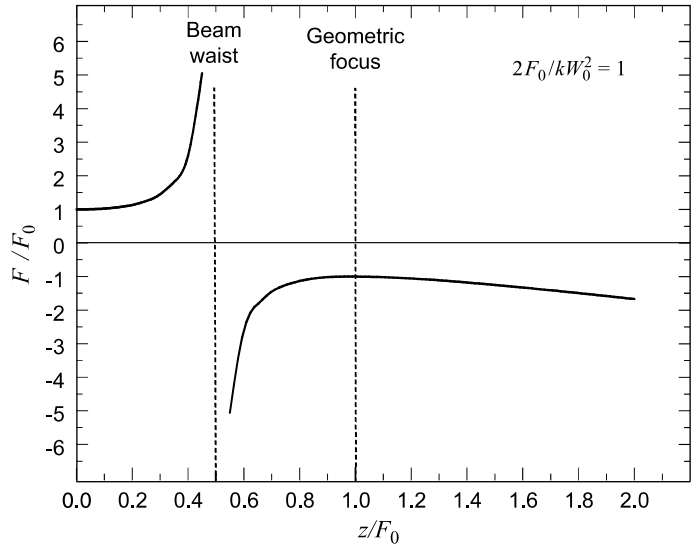

Figure 4.4 Scaled phase front radius of curvature as a function of scaled propagation distance.

sign prior to the beam waist (the minimum beam spot size) and becomes unbounded at the waist (i.e., the phase front is planar). Upon passing through the waist region, the phase front radius of curvature changes sign to negative and remains so for the rest of the path. Also, at the geometric focus the phase front radius of curvature is always the negative of that at the transmitter.

The *irradiance* or *intensity* of the optical wave is the squared magnitude of the field. Thus, at the receiver the irradiance is

$$\begin{aligned} I^0(r,z) &= |U_0(r,z)|^2 \\ &= I^0(0,z)\exp\left(-\frac{2r^2}{W^2}\right), \qquad \left[\mathrm{W/m^2}\right] \end{aligned} \tag{40}$$

where

$$I^0(0,z) = \frac{W_0^2}{W^2} = \frac{1}{\Theta_0^2 + \Lambda_0^2} \tag{41}$$

is the *on-axis irradiance*. Finally, because we assume no loss of power, the total power at the receiver (or transmitter) is

$$P = \int\int_{-\infty}^{\infty} I^0(r,0)d^2r = \int\int_{-\infty}^{\infty} I^0(r,z)d^2r = \frac{1}{2}\pi W_0^2. \quad [\mathrm{W}] \tag{42}$$

4.4.2 Output plane beam parameters

Although the beam characteristics (36)–(38) are well defined using the input plane beam parameters, it is instructive to present a parallel development of these

expressions based on beam parameters at the output plane. We start by writing the complex amplitude A of the Gaussian-beam wave (24) as (now with $a_0 = 1$)

$$A = \frac{1}{1 + i\alpha_0 z} = \frac{1}{\Theta_0 + i\Lambda_0} = \Theta - i\Lambda \tag{43}$$

where the real (nondimensional) parameters Θ and Λ are defined by

$$\Theta = \frac{\Theta_0}{\Theta_0^2 + \Lambda_0^2}, \quad \Lambda = \frac{\Lambda_0}{\Theta_0^2 + \Lambda_0^2}. \tag{44}$$

By doing so, we find that

$$\begin{aligned} \frac{i\alpha_0 z}{1 + i\alpha_0 z} &= 1 - \frac{1}{\Theta_0 + i\Lambda_0} \\ &= 1 - (\Theta - i\Lambda) \\ &= \overline{\Theta} + i\Lambda, \end{aligned}$$

where, in the last step, we have introduced the *complementary* parameter

$$\overline{\Theta} = 1 - \Theta. \tag{45}$$

In terms of parameters Θ and Λ, the optical wave (24) becomes

$$\begin{aligned} U_0(r, z) &= (\Theta - i\Lambda) \exp\left[ikz + \frac{ik}{2z}\left(\overline{\Theta} + i\Lambda\right)r^2\right] \\ &= \sqrt{\Theta^2 + \Lambda^2} \exp\left(-\frac{k\Lambda r^2}{2z}\right) \exp\left[i\left(kz - \varphi + \frac{k\overline{\Theta} r^2}{2z}\right)\right]. \end{aligned} \tag{46}$$

Comparing Eq. (46) with Eq. (35), we deduce that

$$\sqrt{\Theta^2 + \Lambda^2} = \frac{1}{\sqrt{\Theta_0^2 + \Lambda_0^2}}, \quad \frac{1}{W^2} = \frac{k\Lambda}{2z}, \quad \frac{1}{F} = -\frac{\overline{\Theta}}{z}.$$

The last two expressions above identify parameters Θ and Λ as the counterparts of Θ_0 and Λ_0 defined by Eqs. (33), viz.,

$$\Theta = 1 + \frac{z}{F}, \qquad \Lambda = \frac{2z}{kW^2}. \tag{47}$$

Analogous to the input plane beam parameters Θ_0 and Λ_0, the parameters Θ and Λ are called the *output plane* (or *receiver*) *beam parameters.* We further recognize Θ as the *refraction parameter* and Λ as the *diffraction parameter* at the output plane.

In terms of the output plane beam parameters, the longitudinal phase shift (36), spot size (37), and phase front radius of curvature (38) can be expressed as

$$\varphi = \tan^{-1}\frac{\Lambda_0}{\Theta_0} = \tan^{-1}\frac{\Lambda}{\Theta}, \tag{48}$$

$$W = W_0\sqrt{\Theta_0^2 + \Lambda_0^2} = \frac{W_0}{\sqrt{\Theta^2 + \Lambda^2}}, \tag{49}$$

$$F = \frac{F_0\big(\Theta_0^2 + \Lambda_0^2\big)(\Theta_0 - 1)}{\Theta_0^2 + \Lambda_0^2 - \Theta_0} = \frac{F_0\big(\Theta^2 + \Lambda^2 - \Theta\big)}{(\Theta - 1)(\Theta^2 + \Lambda^2)}. \tag{50}$$

Similarly, the irradiance profile becomes

$$I^0(r, z) = \left(\frac{1}{\Theta_0^2 + \Lambda_0^2}\right)\exp\left(-\frac{2r^2}{W^2}\right) = (\Theta^2 + \Lambda^2)\exp\left(-\frac{2r^2}{W^2}\right), \tag{51}$$

where the on-axis irradiance is

$$I^0(0, z) = \frac{W_0^2}{W^2} = \frac{1}{\Theta_0^2 + \Lambda_0^2} = \Theta^2 + \Lambda^2. \tag{52}$$

4.5 Geometrical Interpretations—Part I

In this section the geometric properties of the input plane beam parameters Θ_0 and Λ_0 are developed for line-of-sight propagation in the *complex propagation plane* $p(z) = \Theta_0(z) + i\Lambda_0(z)$. The beam size W_0, radius of curvature F_0, and wavelength $\lambda = 2\pi/k$ are all assumed to be fixed, whereas the path length z is allowed to vary.

For variable propagation path length z, the input plane beam parameters $\Theta_0(z)$ and $\Lambda_0(z)$ are *linear* functions of propagation distance z defined by

$$\begin{aligned} \Theta_0(z) &= 1 - \frac{z}{F_0}, \\ \Lambda_0(z) &= \frac{2z}{kW_0^2}, \end{aligned} \qquad z \geq 0. \tag{53}$$

As such, they represent parametric equations of a *ray-line* in the complex p-plane with parameter z. Thus, starting at $p(0) = 1$ when $z = 0$, this path is traced out by [obtained from (53) by eliminating the parameter z]

$$\Lambda_0 = \Omega_f(1 - \Theta_0), \quad \Lambda_0 \geq 0, \tag{54}$$

where Ω_f is the *focusing parameter* defined by

$$\Omega_f = \frac{2F_0}{kW_0^2}. \tag{55}$$

The numerical value of the parameter Ω_f locates the *geometric focus* of the beam [see Fig. 4.3(*a*)] and $-\Omega_f$ determines the slope of the ray-line (54). Three

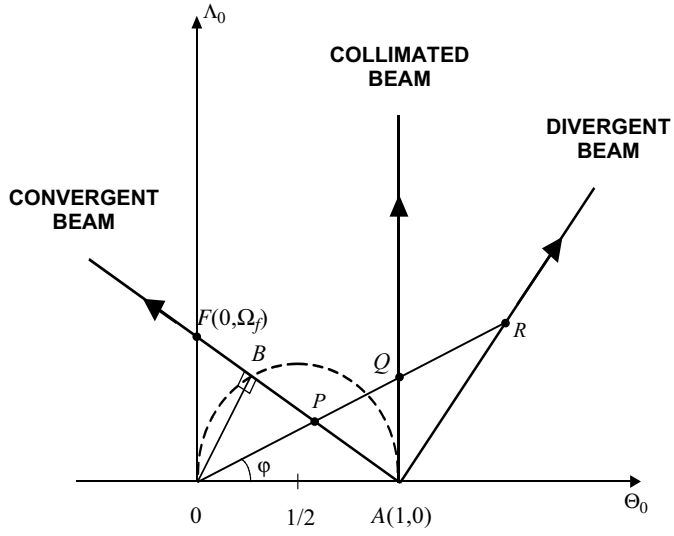

Figure 4.5 Propagation paths in the complex *p*-plane defined by Eq. (54).

possible propagation paths in the *p*-plane are represented in Fig. 4.5, all starting at the point $A(1, 0)$ corresponding to the input plane. An initially convergent beam is represented by the ray-line with negative slope ($\Omega_f > 0$) passing through the geometric focus $F(0, \Omega_f)$ on the positive Λ_0 axis. The vertical ray-line $\Theta_0 = 1$ (with $\Omega_f = \infty$) represents the path of a collimated beam and the remaining ray-line with positive slope ($\Omega_f < 0$) denotes a divergent beam. The geometric focus of a divergent beam occurs prior to the plane $z = 0$. Note that the angle φ at the origin is the phase shift associated with points *P*, *Q*, and *R* on each of the three beam types. Clearly, the geometric focus for a convergent beam occurs when $\varphi = \pi/2$ (90°) and the maximum longitudinal phase shift is $\varphi = \pi$ (180°). For collimated and divergent beams, the maximum longitudinal phase shift is only $\varphi = \pi/2$ (90°).

4.5.1 Beam waist and geometric focus

An arbitrary point $P(\Theta_0, \Lambda_0)$ on any ray-line in Fig. 4.5 defines the phase shift, beam radius, radius of curvature, and on-axis irradiance ($r = 0$) according to Eqs. (36)–(39). The distance from (0, 0) to any point $P(\Theta_0, \Lambda_0)$ on a ray-line is the reciprocal of the beam on-axis amplitude, i.e.,

$$|\overline{0P}| = \sqrt{\Theta_0^2 + \Lambda_0^2} = \frac{1}{|A|}. \tag{56}$$

Hence, the point closest to the origin (0, 0) on the convergent beam ray-line locates the *beam waist* where the amplitude (or irradiance) is maximum. This point, marked *B* in Fig. 4.5, is at the intersection of the normal line drawn from the

origin to the ray-line, and therefore the beam waist always lies on the dashed semicircle shown in Fig. 4.5 with center at (1/2,0).

The distance to the geometric focus $F(0, \Omega_f)$ is $z_f = F_0$ and the beam spot size is

$$W_f = W_0 \Omega_f = \frac{2F_0}{kW_0}. \tag{57}$$

Prior to the geometric focus is the beam waist located at distance (see Prob. 12)

$$z_B = \frac{F_0}{1 + \Omega_f^2}, \tag{58}$$

where the coordinates defining the position of the beam waist B are given by

$$\Theta_{0,B} = \frac{\Omega_f^2}{1 + \Omega_f^2}, \quad \Lambda_{0,B} = \frac{\Omega_f}{1 + \Omega_f^2}. \tag{59}$$

Also, the free-space spot size at the waist ($z = z_B$) is

$$W_B = W_0 \sqrt{\frac{\Omega_f^2}{1 + \Omega_f^2}} = \frac{W_f}{\sqrt{1 + \Omega_f^2}}. \tag{60}$$

From Eqs. (59) we see that $\Lambda_{0,B}$ is bounded by $0 \le \Lambda_{0,B} \le 1/2$ and its maximum value occurs when $\Omega_f = 1$. This critical value of the geometric focus places the beam waist at the maximum distance from the transmitter, which corresponds to $z = F_0/2$ (see Prob. 14 and Fig. 4.4).

4.5.2 Rayleigh range

In some applications it is important to know how fast an ideal Gaussian beam will expand because of diffraction spreading as it propagates away from the waist region. The distance at which the beam travels from the waist before the beam area spot size doubles [i.e., $W = \sqrt{2} W_B$] is called the *Rayleigh range*. For a collimated beam the Rayleigh range is characterized by $0 \le \Lambda_0 \le 1$, representing a $\pi/4$ (45°) phase shift in φ. In addition, in the case of a collimated beam, the distance $z_R = 0.5\, kW_0^2$ (at which $\Lambda_0 = 1$) forms a dividing line between the *near-field* (*near-Fresnel region*) and the *far-field* (*Fraunhofer region*). In the case of an initially convergent beam, the Rayleigh range represents a $\pi/2$ (90°) phase shift and extends on both sides of the beam waist bounded by

$$z_{R_1} \le z \le z_{R_2}: \quad z_{R_1} = \frac{F_0(1 - \Omega_f)}{1 + \Omega_f^2}, \quad z_{R_2} = \frac{F_0(1 + \Omega_f)}{1 + \Omega_f^2}. \tag{61}$$

Geometrically, the Rayleigh range lies between points P_1 and P_2 on the circle centered at the beam waist B and passing through the origin as shown in Fig. 4.6.

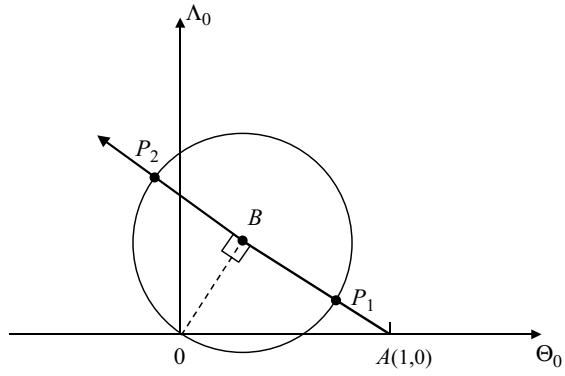

Figure 4.6 Rayleigh range designated by points P_1 and P_2 at the intersection of the propagation ray-line and the circle centered at the beam waist B and passing through the origin.

4.6 Geometrical Interpretations—Part II

The on-axis complex amplitude A at the output plane of a lowest-order Gaussian-beam wave is related to the propagation parameter p through the relationship (with $a_0 = 1$)

$$A = \frac{1}{p} = \Theta - i\Lambda. \tag{62}$$

Equation (62) represents a *conformal transformation* that maps "lines not passing through the origin" in the complex p-plane into "circles through the origin" in the complex A-plane [16,17]. Thus, the propagation paths discussed in Section 4.5 can also be studied in the complex amplitude plane using output plane beam parameters Θ and Λ.

4.6.1 Beam waist and geometric focus

Under the conformal mapping (62) any propagation path described by the ray-line (54) becomes a portion of a circle described by

$$\Theta^2 + \Lambda^2 = \Theta + \frac{\Lambda}{\Omega_f}, \tag{63}$$

or, equivalently, by

$$\left(\Theta - \frac{1}{2}\right)^2 + \left(\Lambda - \frac{1}{2\Omega_f}\right)^2 = \frac{W_0^2}{4W_B^2}, \quad \Lambda \geq 0. \tag{64}$$

Special cases of Eq. (64) shown in Fig. 4.7 represent the three propagation ray-lines in Fig. 4.5. Note that, because three points uniquely define a circle, and

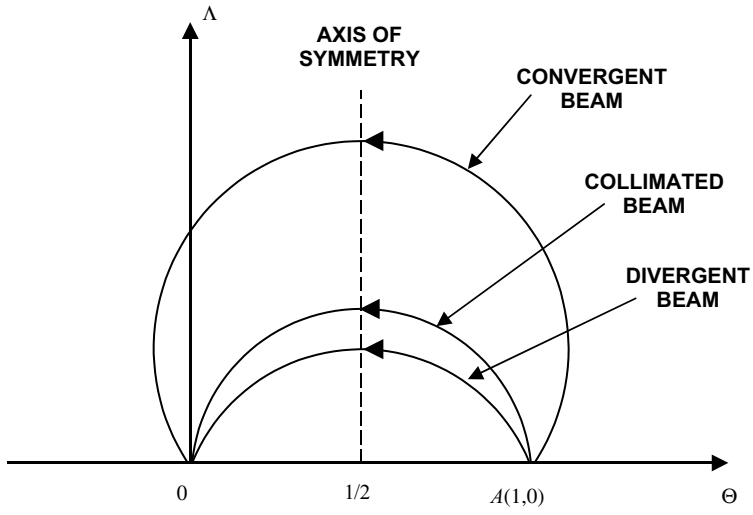

Figure 4.7 Propagation paths in the complex A-plane corresponding to those in Fig. 4.5 under the conformal mapping $A = 1/p$.

$(0, 0)$ and $(1, 0)$ are two points always on the circle, only one additional point $P(\Theta, \Lambda)$ is necessary to define all properties of any Gaussian beam uniquely.

The circle for a convergent beam ($\Omega_f > 0$) is reproduced in Fig. 4.8. The center of this circle is located at $C(1/2, 1/(2\Omega_f))$, and its diameter W_0/W_B is the free-space on-axis amplitude of the beam at the waist. When $z = 0$, the propagation path begins at $A(1, 0)$ and moves counterclockwise around the circle as the path length increases. The point $P(\Theta, \Lambda)$ on the circle, representing an arbitrary

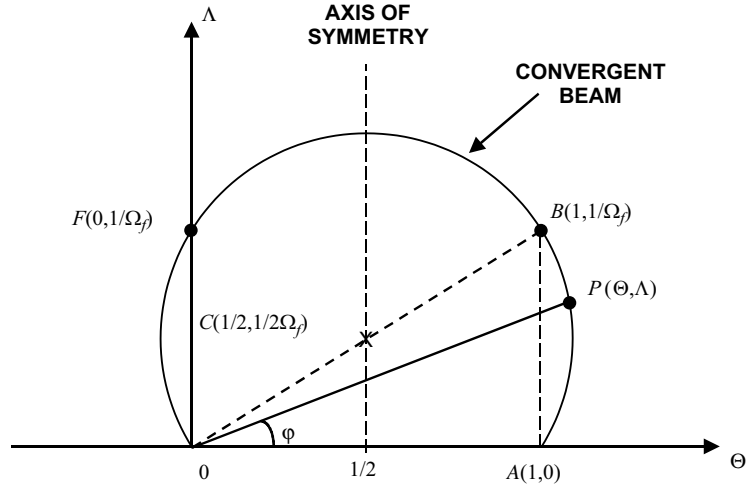

Figure 4.8 Propagation path in the complex A-plane corresponding to an initially convergent beam. Point $A(1,0)$ is the initial point $z = 0$, B is the beam waist, and F is the geometric focus.

plane along the path, identifies the longitudinal phase shift, beam radius, phase front radius of curvature, and on-axis irradiance according to Eqs. (48) through (51). Thus, the length of the line segment from 0 to P equals the on-axis amplitude (square root of the irradiance)

$$|\overline{0P}| = \sqrt{\Theta^2 + \Lambda^2} = |A|, \tag{65}$$

whereas the angle φ at the origin is the longitudinal phase shift. The beam waist is located at $B(1, 1/\Omega_f)$, where $\Theta = 1$ once again, and the geometric focus is at $F(0, 1/\Omega_f)$, where $\Theta = 0$ (i.e., $F = -F_0$). Last, in addition to Eqs. (49) and (50), the spot radius and radius of curvature in the complex amplitude plane have the representations

$$W = \frac{W_0}{\sqrt{\Theta + \Lambda/\Omega_f}}, \quad F = \frac{F_0}{\Theta - \Omega_f \Lambda}. \tag{66}$$

As $\Omega_f \to \infty$, the center of the circle in Fig. 4.8 approaches the point $(1/2, 0)$ on the Θ-axis, depicting the propagation of a collimated beam. In this case the beam waist and geometric focus merge with the initial point $A(1, 0)$ and terminal point $(0, 0)$, respectively, of the propagation path.

4.7 Higher-Order Gaussian-Beam Modes

The majority of studies of wave propagation has involved the lowest-order Gaussian-beam or TEM_{00} mode. For example, in Section 4.3 we showed that the lowest order Gaussian-beam mode is a solution of the paraxial wave equation (9). In practice, however, there are certain scenarios when it is desirable to minimize the excitation of nonlinearities within the crystal of a laser or when the received optical wave needs to have a multiple spot pattern. In those cases, the higher-order solutions of the paraxial wave equation can be used to generate *higher-order Gaussian-beam modes* with Hermite polynomials (CO_2 laser) in rectangular coordinates or Laguerre polynomials (HeNe laser) in cylindrical coordinates (see [4]).

4.7.1 Hermite-Gaussian beams

The higher-order *Hermite-Gaussian modes* TEM_{mn} of a collimated beam at the exit aperture of a laser are described by

$$z = 0: \quad U_{mn}(x, y, 0) = H_m\left(\frac{\sqrt{2}x}{W_{x,0}}\right) H_n\left(\frac{\sqrt{2}y}{W_{y,0}}\right) \exp\left(-\frac{x^2}{W_{x,0}^2} - \frac{y^2}{W_{y,0}^2}\right) \tag{67}$$

where $m, n = 0, 1, 2, \ldots$, the TEM_{00} spot size along the x- and y-axes at the transmitter is given by $W_{x,0}$ and $W_{y,0}$, respectively, and $H_n(x)$ is the nth Hermite polynomial. However, the higher-order modes always form a pattern of spots

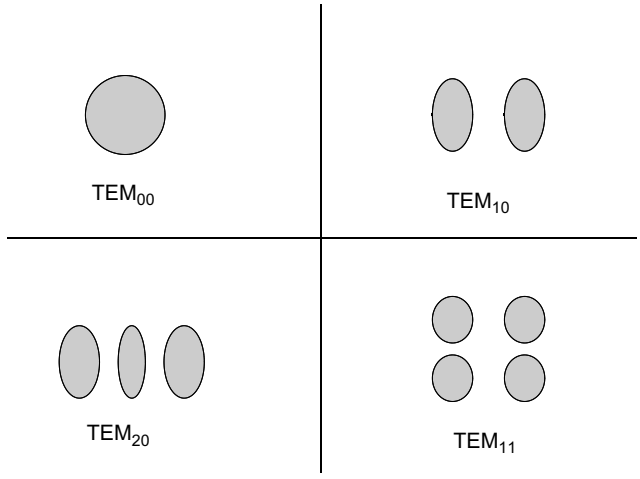

Figure 4.9 Illustrations depiciting various mode patterns (light spots) associated with some of the higher-mode Hermite-Gaussian beams.

for the irradiance (see Figs. 4.9–4.11) rather than a single spot as exhibited by the TEM_{00} mode.

4.7.2 Paraxial equation: direct solution method

To find the field at propagation distance z from the transmitter, we can once again solve the paraxial wave equation (9). We begin by assuming the solution of the paraxial wave equation can be expressed in the product form

$$V(x, y, z) = v(x, z)w(y, z), \tag{68}$$

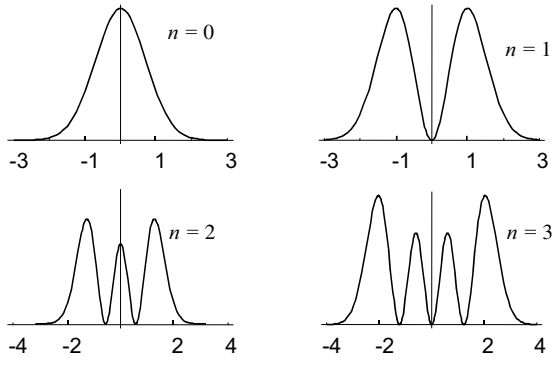

Figure 4.10 Cross-sectional view of higher-mode Hermite-Gaussian beams.

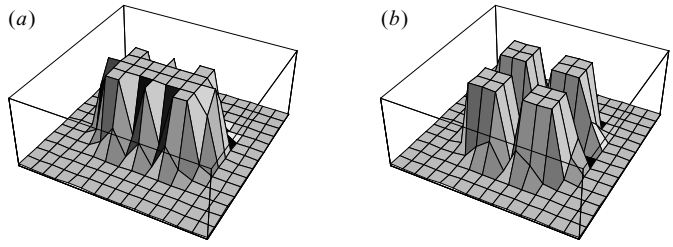

Figure 4.11 Three-dimensional irradiance plot of higher-order Hermite-Gaussian modes (*a*) TEM_{20} and (*b*) TEM_{11}.

where each function on the right-hand side of (68) has the same mathematical form. In the x transverse coordinate, the paraxial wave equation becomes

$$\frac{\partial^2 v}{\partial x^2} + 2ik\frac{\partial v}{\partial z} = 0. \tag{69}$$

An identical equation in w and y describes the paraxial wave equation in the y direction.

To solve Eq. (69), we look for solutions of the form

$$v(x,z) = A(z)H\left[\frac{x}{q(z)}\right]\exp\left[-\frac{\alpha_0 k x^2}{2p(z)}\right], \tag{70}$$

where $A(z)$, $q(z)$, and $H(x/q)$ are unknown functions and $p(z) = 1 + i\alpha_0 z$ is the same as that for a lowest-order Gaussian-beam wave. The direct substitution of (70) into (69) yields the expression

$$H'' - 2\left(\frac{x}{q}\right)\left(\frac{\alpha_0 k q^2}{p} + ikqq'\right)H' + q^2\left(\frac{2ikA'}{A} - \frac{\alpha_0 k}{p}\right)H + x^2q^2\left[\left(\frac{\alpha_0 k}{p}\right)^2 + \frac{i\alpha_0 k^2 p'}{p^2}\right]H = 0. \tag{71}$$

From the definition of $p(z)$, the last term in brackets (with coefficient x^2q^2) vanishes. To reduce the remaining equation in H to Hermite's differential equation of order m, we require that

$$\frac{\alpha_0 k q^2}{p} + ikqq' = 1 \tag{72}$$

and

$$\frac{2ikA'}{A} - \frac{\alpha_0 k}{p} = \frac{2m}{q^2}. \tag{73}$$

Under these conditions, Eq. (71) reduces to

$$H_m'' - 2\left(\frac{x}{q}\right)H_m' + 2mH_m = 0, \quad m = 0, 1, 2, \ldots, \tag{74}$$

which we recognize as *Hermite's equation* [6] with the *Hermite polynomials* $H_m(x/q)$ as solutions.

The Hermite-Gaussian functions we wish to derive here are the most widely used higher-order solutions of the paraxial wave equation [3], but not the only solutions [4]. To obtain these desired functions, we first recognize that one possible solution of (72) is

$$q(z) = \frac{W(z)}{\sqrt{2}}, \tag{75}$$

where we made use of the identity $\partial W/\partial z = -W/F$ (see Prob. 8). Next, by recognizing the relation $\alpha_0 k/p = -ikp'/p$, we find that Eq. (73) takes the form

$$\frac{2ikA'}{A} + \frac{ikp'}{p} = \frac{2m}{q^2}. \tag{76}$$

Without providing the details, it can be shown that the solution of this last equation is

$$A(z) = \frac{1}{\sqrt{p(z)}} \exp[i\varphi(z)], \tag{77}$$

where $\varphi(z)$ is an unimportant phase factor. Combining results, we have

$$v_m(x,z) = \frac{1}{\sqrt{p_x(z)}} H_m\left(\frac{\sqrt{2}x}{W_x}\right) \exp\left(-\frac{x^2}{W_x^2} - i\frac{kx^2}{2F_x}\right) \exp[i\varphi_m(z)], \quad m = 0, 1, 2, \ldots, \tag{78}$$

where the subscript x has been introduced in (78) to identify the parameters in the x transverse direction and $W_x = W_x(z)$. In the y direction, the solution has an identical form, which combined with (78) leads to

$$\begin{aligned} V_{mn}(x,y,z) &= v_m(x,z) w_n(y,z) \\ &= \frac{1}{\sqrt{p_x(z)p_y(z)}} H_m\left(\frac{\sqrt{2}x}{W_x}\right) H_n\left(\frac{\sqrt{2}y}{W_y}\right) \\ &\quad \times \exp\left(-\frac{x^2}{W_x^2} - \frac{y^2}{W_y^2} - i\frac{kx^2}{2F_x} - i\frac{ky^2}{2F_y}\right) \exp[i\varphi_m(z) + i\varphi_n(z)]; \\ &\qquad\qquad m, n = 0, 1, 2, \ldots. \end{aligned} \tag{79}$$

It is customary in many cases to assume the parameters in both x and y directions are the same. For example, we may set

$$W_x(z) = W_y(z) = W(z), \tag{80}$$

where $W(z)$ is the spot size of the lowest-order Gaussian-beam wave. However, because higher-order beams always form a pattern of spots (see Fig. 4.9), rather than a single spot of light, we need a new definition of spot size of these

higher-order modes. Carter [18] suggests that the spot size of the pth mode be defined by

$$\sigma_{s,p}^2(z) = \frac{4\int\int_{-\infty}^{\infty} s^2 I_{mn}(x,y,z)\,dx\,dy}{\int\int_{-\infty}^{\infty} I_{mn}(x,y,z)\,dx\,dy}, \tag{81}$$

where s represents either x or y and p denotes either m or n. (Because Carter's definition of spot size is slightly different, we need a factor of 4 in the numerator instead of 2.) Based on (79), it follows that the irradiance of the Hermite-Gaussian beam is given by

$$I_{mn}(x,y,z) = \frac{W_{x,0}W_{y,0}}{W_x W_y} H_m^2\left(\frac{\sqrt{2}x}{W_x}\right) H_n^2\left(\frac{\sqrt{2}y}{W_y}\right) \exp\left(-\frac{2x^2}{W_x^2} - \frac{2y^2}{W_y^2}\right); \quad m,n = 0,1,2,\ldots. \tag{82}$$

By substituting (82) into (81), we find that the "effective spot size" is given by the rectangular domain $\sigma_{x,m}(z) \times \sigma_{y,n}(z)$, where

$$\begin{aligned} \sigma_{x,m}(z) &= \sqrt{2m+1}\,W_x(z), \quad m = 0,1,2,\ldots, \\ \sigma_{y,n}(z) &= \sqrt{2n+1}\,W_y(z), \quad n = 0,1,2,\ldots. \end{aligned} \tag{83}$$

4.7.3 Paraxial equation: Huygens-Fresnel integral

A more direct approach to finding the field of a Hermite-Gaussian beam at distance z from the transmitter is to use the Huygens-Fresnel integral [4]

$$U_{mn}(x,y,z) = -\frac{ik}{2\pi z}\exp(ikz)\int\int_{-\infty}^{\infty} U_{mn}(\xi,\eta,0) \times \exp\left[\frac{ik}{2z}(\xi - x)^2\right]\exp\left[\frac{ik}{2z}(\eta - y)^2\right]d\xi\,d\eta. \tag{84}$$

By substituting the field (67) into (84), routine integration yields the solution

$$U_{mn}(x,y,z) = V_{mn}(x,y,z)\exp(ikz), \tag{85}$$

where $V_{mn}(x,y,z)$ is defined by Eq. (79). We leave it to the reader to show that (85) for the special case given by (80) can also be expressed in terms of output plane Gaussian-beam parameters according to (see Prob. 25)

$$U_{mn}(x,y,z) = (\Theta - i\Lambda)\left(\frac{\Theta - i\Lambda}{\Theta + i\Lambda}\right)^{(m+n)/2} H_m\left(\frac{\sqrt{2}x}{W}\right) H_n\left(\frac{\sqrt{2}y}{W}\right) \times \exp\left[ikz + \frac{ik}{2z}\left(\overline{\Theta} + i\Lambda\right)\left(x^2 + y^2\right)\right]. \tag{86}$$

4.7.4 Laguerre-Gaussian beams

By assuming cylindrical symmetry, higher-order modes of a collimated beam at the exit aperture ($z = 0$) of a laser can be described in cylindrical coordinates (r, θ, z) by

$$z = 0: \quad U_{mn}(r, \theta, 0) = \left(\frac{\sqrt{2}r}{W_0}\right)^m (-i)^m \exp(im\theta) \exp\left(-\frac{r^2}{W_0^2}\right) L_n^{(m)}\left(\frac{2r^2}{W_0^2}\right), \quad (87)$$

where $\mathbf{r}$ is a vector in the transverse plane at angle θ, W_0 is the radius of the TEM_{00} mode beam, $L_n^m(x)$ is the *associated Laguerre polynomial*, and n and m are the radial and angular mode numbers.

The field described by (87) is called a *Laguerre-Gaussian beam.* By using the Huygens-Fresnel integral (25), it can be shown that the field of the Laguerre-Gaussian beam at distance z from the transmitter is given by

$$U_{mn}(r, \theta, z) = C_{mn} \frac{W_0}{W} \left(\frac{\sqrt{2}r}{W(z)}\right)^m L_n^{(m)}\left(\frac{2r^2}{W^2(z)}\right) \times \exp[-i(2n + m + 1)\varphi(z)] \exp\left(ikz + im\theta - \frac{r^2}{W^2} - i\frac{kr^2}{2F}\right); \quad m, n = 0, 1, 2, \ldots, \quad (88)$$

where C_{mn} is an unimportant phase constant, and W and F denote the spot size and phase front radius of curvature for a TEM_{00} beam.

The irradiance deduced from (88) is

$$I(r, \theta, z) = |U_{mn}(r, \theta, z)|^2 = \frac{W_0^2}{W^2} \left(\frac{2r^2}{W^2}\right)^m \left[L_n^{(m)}\left(\frac{2r^2}{W^2}\right)\right]^2 \exp\left(-\frac{2r^2}{W^2}\right). \quad (89)$$

The spot pattern for Laguerre-Gaussian functions consists of multiple rings as illustrated in Figs. 4.12 and 4.13. Following Carter [18], Phillips and Andrews

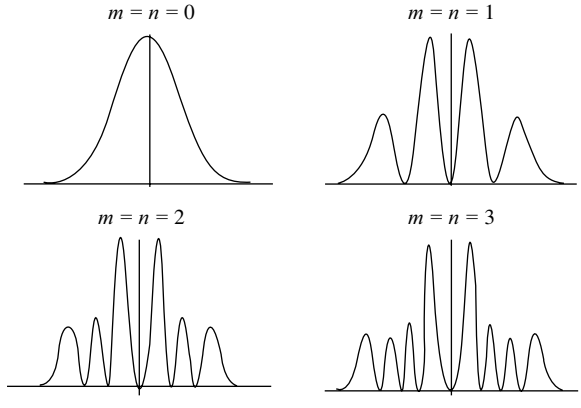

Figure 4.12 Cross-sectional view of higher-mode Laguerre-Gaussian beams.

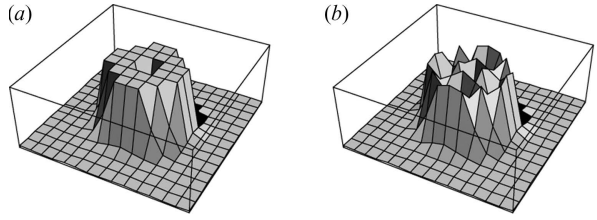

Figure 4.13 Three-dimensional irradiance plot of higher-order Laguerre-Gaussian modes (*a*) TEM_{20} and (*b*) TEM_{11}.

[19] have shown that using an expression like (81) with the irradiance defined by (89), a comparable spot size associated with a Laguerre-Gaussian beam can be defined by

$$\sigma_{mn}(z) = \sqrt{2n + m + 1}W(z); \qquad m, n = 0, 1, 2, \ldots. \tag{90}$$

The significance of this definition for spot size and that in (83) is that the spot size so defined contains all the irradiance maxima of the various polynomials.

4.8 *ABCD* Ray-Matrix Representations

An effective way to discuss Gaussian-beam wave propagation through various optical structures like lenses and apertures is by use of 2×2 matrices known as *ABCD ray matrices.* The use of such matrices allows us to describe the propagation of a Gaussian beam through a train of optical elements by utilizing the cascade scheme of multiplying successive matrix representations of each optical element, including those that describe the free-space path between optical elements [4]. In this fashion the entire propagation path, consisting of various optical elements at arbitrary positions along the propagation path, can be represented by a single *ABCD* ray matrix. As in previous sections, we invoke the paraxial approximation, which is valid when the separation distance between optical elements is large compared with the transverse extent of the beam.

The notion of a ray matrix is most easily understood by examining a one-dimensional analog. Consider a ray of light propagating between two points denoted by r_1 and r_2 in parallel transverse planes at $z = z_1$ and $z = z_2$ separated by distance L (see Fig. 4.14). The angle that the light ray makes from point r_1 to point r_2 is ϕ, for which

$$\tan\phi = \frac{r_2 - r_1}{L} = \frac{dr_1}{dz}. \tag{91}$$

Rewriting Eq. (91), we have

$$r_2 = r_1 + L\frac{dr_1}{dz} = r_1 + Lr_1', \tag{92}$$

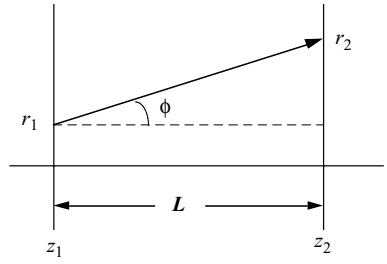

Figure 4.14 Line-of-sight section of length L.

and recognizing that the slope at r_1 is the same as that at r_2 yields

$$r_2' = r_1'. \tag{93}$$

By combining (92) and (93), we obtain the matrix equation

$$\begin{pmatrix} r_2 \\ r_2' \end{pmatrix} = \begin{pmatrix} 1 & L \\ 0 & 1 \end{pmatrix} \begin{pmatrix} r_1 \\ r_1' \end{pmatrix}. \tag{94}$$

The 2×2 matrix on the right-hand side of (94) is the *ABCD* ray matrix depicting free-space propagation over a path of length L. If we formally replace r_1 and r_2 with vectors $\mathbf{r}_1$ and $\mathbf{r}_2$, the same relation holds for rotationally symmetric systems. Other *ABCD* matrices for a thin lens and finite aperture stop with rotational symmetry are listed in Table 4.1. Note that the finite aperture stop, representing a "soft aperture," has a complex matrix element. This type of aperture is approximated by a Gaussian function and thus is also called a *Gaussian aperture.*

An important property of all ray matrices listed in Table 4.1 is that

$$AD - BC = 1, \tag{95}$$

Table 4.1 Ray matrices for various optical elements.

Structure	Matrix
Line-of-sight section (length L)	$\begin{pmatrix} 1 & L \\ 0 & 1 \end{pmatrix}$
Thin lens (focal length F_G)	$\begin{pmatrix} 1 & 0 \\ -1/F_G & 1 \end{pmatrix}$
Finite aperture stop (aperture radius W_G)	$\begin{pmatrix} 1 & 0 \\ 2i/kW_G^2 & 1 \end{pmatrix}$
Gaussian lens (thin lens and aperture stop)	$\begin{pmatrix} 1 & 0 \\ -1/F_G + 2i/kW_G^2 & 1 \end{pmatrix}$

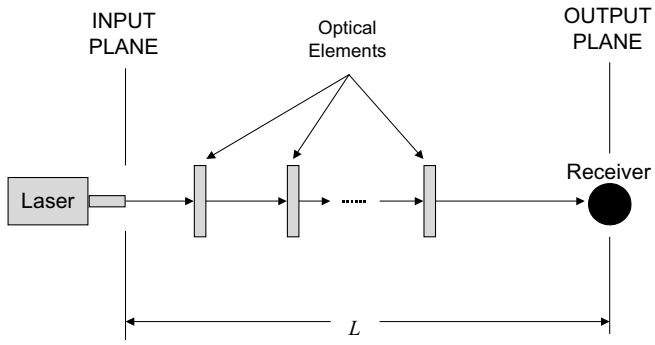

Figure 4.15 A ray-matrix optical system in cascade.

which is valid as long as input and output planes are in the same medium. Although we confine our attention here to systems featuring rotational symmetry, we should point out that *ABCD* ray matrices have also been developed for rectangular systems [4].

Let us now consider an optical ray propagating through a sequence of rotationally symmetric optical elements (plus straight line sections between the elements) all properly aligned and arranged in cascade fashion as illustrated in Fig. 4.15. By representing each optical element and straight line section along the propagation path by its *ABCD* matrix, the overall *ABCD* matrix for N such matrices is obtained from the product

$$\begin{pmatrix} A & B \\ C & D \end{pmatrix} = \begin{pmatrix} A_N & B_N \\ C_N & D_N \end{pmatrix} \begin{pmatrix} A_{N-1} & B_{N-1} \\ C_{N-1} & D_{N-1} \end{pmatrix} \cdots \begin{pmatrix} A_1 & B_1 \\ C_1 & D_1 \end{pmatrix}. \tag{96}$$

Note that the matrices in (96) must be arranged in reverse order from the order of occurrence.

4.8.1 Paraxial approximation for *ABCD* optical systems

When optical elements are present along the propagation path as shown in Fig. 4.15, the slopes r_1' and r_2' at the beginning and end of the path are no longer related by the simple relation (93). For example, under a general *ABCD* optical system, we have

$$\begin{pmatrix} r_2 \\ r_2' \end{pmatrix} = \begin{pmatrix} A & B \\ C & D \end{pmatrix} \begin{pmatrix} r_1 \\ r_1' \end{pmatrix} = \begin{pmatrix} Ar_1 + Br_1' \\ Cr_1 + Dr_1' \end{pmatrix}, \tag{97}$$

from which we deduce

$$\begin{aligned} r_1' &= \frac{1}{B}(r_2 - Ar_1), \\ r_2' &= Cr_1 + Dr_1' = Cr_1 + \frac{D}{B}(r_2 - Ar_1). \end{aligned} \tag{98}$$

However, by using $AD - BC = 1$, we find that the second equation in (98) becomes

$$r_2' = \frac{1}{B}(Dr_2 - r_1). \tag{99}$$

In addition, the paraxial approximation (7) must be generalized to account for the small path changes induced by the optical elements.

To begin, let us review the *one-dimensional geometry* associated with the free-space line-of-sight paraxial approximation as shown in Fig. 4.14 and redrawn in Fig. 4.16. If we assume an optical ray begins at point O in the plane $z = z_1$ with position r_1 above the optical axis and ends up at point T in the plane $z = z_2$ with position r_2 above the optical axis, then the paraxial approximation given by (7) leads to the expression

$$R \cong L + \frac{1}{2L}(r_2 - r_1)^2 = L + \Delta L, \quad |r_2 - r_1| \ll L, \tag{100}$$

where $R = |\overline{\mathrm{OT}}|, L = |\overline{\mathrm{OP}}| = |\overline{\mathrm{OS}}|$, and

$$\Delta L = \frac{1}{2L}(r_2 - r_1)^2. \tag{101}$$

Using the geometry of Fig. 4.16, we can also express $\Delta L = |\overline{\mathrm{ST}}|$ in terms of the slopes r_1' and r_2'. That is, although not exact, the distance line $|\overline{\mathrm{QT}}| \cong 2\Delta L$ so that the angle ϕ in triangle ΔPQT satisfies

$$\sin\phi = \frac{|\overline{\mathrm{QT}}|}{r_2 - r_1} \cong \frac{2\Delta L}{r_2 - r_1}. \tag{102}$$

Consequently, using the small angle approximation $\sin\phi \cong \tan\phi$, we are led to

$$\Delta L \cong \frac{1}{2}(r_2 - r_1)\tan\phi \cong \frac{1}{2}(r_2 r_2' - r_1 r_1'), \tag{103}$$

which follows by use of (91) and recognizing that angle ϕ in triangle ΔPOT in Fig. 4.16 is the same as that for ΔQPT.

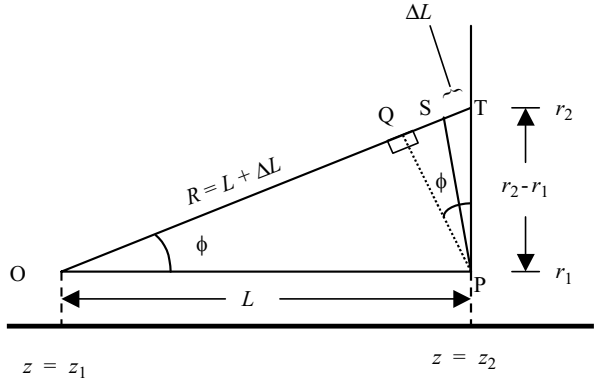

Figure 4.16 Geometry associated with the paraxial approximation.

If we now substitute r_1' and r_2' from (98) and (99) into (103), we find that

$$\Delta L \cong \frac{1}{2}(r_2 r_2' - r_1 r_1') \cong \frac{1}{2B}[r_2(Dr_2 - r_1) - r_1(r_2 - Ar_1)]. \tag{104}$$

Thus, the overall path length, or *eikonal function* $\rho(r_1, r_2)$, of an optical ray passing through an *ABCD* optical system from position r_1 in the plane at $z = z_1$ to position r_2 in the plane at $z = z_2$ leads to a more general form of the paraxial approximation described by

$$\rho(r_1, r_2) \cong L + \Delta L \cong L + \frac{1}{2B}\left(Ar_1^2 - 2r_1 r_2 + Dr_2^2\right). \tag{105}$$

4.8.2 Generalized Huygens-Fresnel integral

Using the *ABCD* matrix representation for the propagation channel between input and output planes separated by distance L, the Green's function [Eq. (26)] in the Huygens-Fresnel integral [Eq. (25)] assumes the more general form [4]

$$\begin{aligned} G(\mathbf{s}, \mathbf{r}; L) &= \frac{1}{4\pi B}\exp[ik\rho(\mathbf{s}, \mathbf{r})] \\ &= \frac{1}{4\pi B}\exp\left[ikL + \frac{ik}{2B}\left(As^2 - 2\mathbf{s}\cdot\mathbf{r} + Dr^2\right)\right], \end{aligned} \tag{106}$$

which follows from the result of Eq. (105) extended to a rotationally symmetric system. The factor $1/4\pi B$ in front is necessary for power conservation. In terms of this more general Green's function, we obtain the *generalized Huygens-Fresnel integral*

$$U_0(\mathbf{r}, L) = -\frac{ik}{2\pi B}\exp(ikL)\int\int_{-\infty}^{\infty} d^2 s U_0(\mathbf{s}, 0)\exp\left[\frac{ik}{2B}\left(As^2 - 2\mathbf{s}\cdot\mathbf{r} + Dr^2\right)\right]. \tag{107}$$

Note that when $A = D = 1$ and $B = L$, Eq. (107) reduces to the standard form of the Huygens-Fresnel integral (25).

Following the notation introduced in Section 4.3.2, the optical field of a lowest-order Gaussian-beam wave at the emitting aperture of a transmitter in the plane $z = 0$ can be characterized by (assuming unit amplitude)

$$U_0(\mathbf{r}, 0) = \exp\left(-\frac{1}{2}\alpha_0 k r^2\right), \tag{108}$$

where α_0 is the complex parameter (15). Here, k is the optical wave number, W_0 is the effective beam radius, and F_0 is the phase front radius of curvature. Let us consider the case in which the Gaussian beam (108) is propagated through a train of optical elements that can all be characterized by a single *ABCD* ray matrix (96). For a rotationally symmetric optical system, the field of the wave at the output

plane ($z = L$) can be described by the generalized Huygens-Fresnel integral (107), which leads to

$$\begin{aligned} U_0(\mathbf{r}, L) &= -\frac{ik}{2\pi B}\exp(ikL)\int\int_{-\infty}^{\infty} d^2s \exp\left(-\frac{1}{2}\alpha_0 k s^2\right) \\ &\quad \times \exp\left[\frac{ik}{2B}(As^2 - 2\mathbf{s}\cdot\mathbf{r} + Dr^2)\right] \\ &= \frac{1}{p(L)}\exp(ikL)\exp\left[-\frac{1}{2}\alpha(L)kr^2\right], \end{aligned} \tag{109}$$

where A, B, C, and D are the ray-matrix elements that characterize the overall propagation path between input and output planes, and

$$p(L) = A + i\alpha_0 B, \tag{110}$$

$$\alpha(L) = \frac{\alpha_0 D - iC}{A + i\alpha_0 B} = \frac{2}{kW^2} + i\frac{1}{F}. \tag{111}$$

The quantities $W = \sqrt{2/\mathrm{Re}[k\alpha(L)]}$ and $F = 1/\mathrm{Im}[\alpha(L)]$ are, respectively, the beam radius and phase front radius of curvature of the wave at the output plane, and Re and Im denote the real and imaginary parts of the argument. By introducing the *generalized output plane Gaussian-beam parameters*

$$\begin{aligned} \Theta &= \mathrm{Re}\left(D + \frac{B}{F} - i\frac{2B}{kW^2}\right), \\ \Lambda &= -\mathrm{Im}\left(D + \frac{B}{F} - i\frac{2B}{kW^2}\right), \end{aligned} \tag{112}$$

the optical field (109) in the presence of a train of optical elements along the propagation path can be expressed in the same form as that for line-of-sight propagation, i.e.,

$$U_0(\mathbf{r}, L) = (\Theta - i\Lambda)\exp(ikL)\exp\left(-\frac{r^2}{W^2} - i\frac{kr^2}{2F}\right). \tag{113}$$

As before, the quantity $\Theta - i\Lambda = 1/p(L)$ describes the complex on-axis amplitude of the beam in the output plane (receiver) at distance L from the input plane (transmitter).

4.9 Single Element Optical System

Complex optical systems where optical elements exist in various planes along the propagation path between input and output planes have important applications in astronomy, optical communication, laser radar (lidar), imaging, and remote sensing. For our analysis of such systems, we concentrate on optical systems having a single optical element between the input and output planes.

4.9.1 Gaussian lens

Let us consider the optical system shown in Fig. 4.17 consisting of a finite *Gaussian lens* (i.e., a thin lens and Gaussian limiting aperture) located at $z = L_1$ between input and output planes. The Gaussian lens has effective aperture radius W_G, focal length F_G, and the distance from the lens to the output plane is L_2, creating a total path length of $L = L_1 + L_2$. Other optical systems featuring a single optical element can be treated similar to that below (e.g., see Chap. 10).

By characterizing the Gaussian lens by the complex parameter

$$\alpha_G = \frac{2}{kW_G^2} + i\frac{1}{F_G}, \tag{114}$$

the overall *ABCD* ray matrix for the optical system shown in Fig. 4.17 is described by

$$\begin{aligned}\begin{pmatrix} A & B \\ C & D \end{pmatrix} &= \begin{pmatrix} 1 & L_2 \\ 0 & 1 \end{pmatrix}\begin{pmatrix} 1 & 0 \\ i\alpha_G & 1 \end{pmatrix}\begin{pmatrix} 1 & L_1 \\ 0 & 1 \end{pmatrix} \\ &= \begin{pmatrix} 1 + i\alpha_G L_2 & L_1 + L_2(1 + i\alpha_G L_1) \\ i\alpha_G & 1 + i\alpha_G L_1 \end{pmatrix}.\end{aligned} \tag{115}$$

From the above expression, it follows that

$$\begin{aligned}p(L_1 + L_2) &= A + i\alpha_0 B \\ &= 1 + i\alpha_0 L_1 + i\alpha_0 L_2 + i\alpha_G L_2(1 + i\alpha_0 L_1).\end{aligned} \tag{116}$$

For the Gaussian-beam wave between transmitter and lens, it is convenient to rewrite the *input plane beam parameters* (33) according to (see Fig. 4.17)

$$\Theta_0 = 1 - \frac{L_1}{F_0}, \quad \Lambda_0 = \frac{2L_1}{kW_0^2}, \tag{117}$$

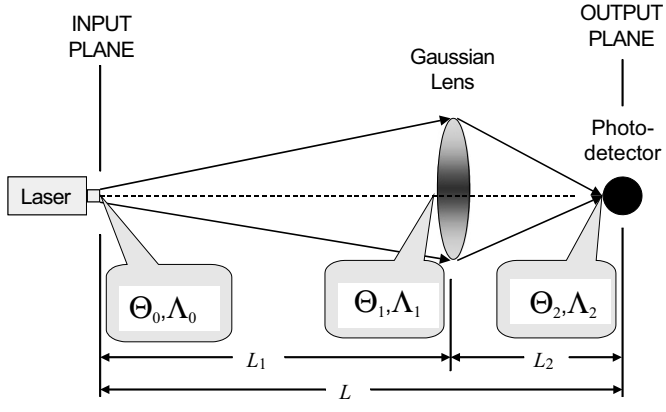

Figure 4.17 Propagation geometry for a Gaussian beam propagating through a Gaussian lens.

which are the real and imaginary parts of $p(L_1) = 1 + i\alpha_0 L_1$. The Gaussian-beam parameters Θ_1 and Λ_1 of the wave incident on the lens are related to the input plane beam parameters by

$$\Theta_1 - i\Lambda_1 = \frac{1}{1 + i\alpha_0 L_1} = \frac{1}{\Theta_0 + i\Lambda_0}, \tag{118}$$

from which we deduce

$$\begin{aligned} &\Theta_1 = \frac{\Theta_0}{\Theta_0^2 + \Lambda_0^2}, \quad \Lambda_1 = \frac{\Lambda_0}{\Theta_0^2 + \Lambda_0^2}, \\ &\overline{\Theta}_1 = 1 - \Theta_1. \end{aligned} \tag{119}$$

Thus, we see that beam parameters (119) are related to the input plane beam parameters (117) in the same fashion as Θ and Λ in Section 4.4.2. Moreover, by writing

$$\begin{aligned} \frac{1}{p(L_1 + L_2)} &= \frac{1}{(1 + i\alpha_0 L_1)[1 + i\alpha_0 L_2/(1 + i\alpha_0 L_1) + i\alpha_G L_2]} \\ &= \frac{\Theta_1 - i\Lambda_1}{1 + (\overline{\Theta}_1 + i\Lambda_1)L_2/L_1 + i\alpha_G L_2}, \end{aligned} \tag{120}$$

the beam spot size W and phase front radius of curvature F at the output plane $z = L_1 + L_2$ can similarly be described by beam parameters Θ_2 and Λ_2, related to Θ_1 and Λ_1 by

$$\Theta_2 - i\Lambda_2 = \frac{1}{1 + (\overline{\Theta}_1 + i\Lambda_1)L_2/L_1 + i\alpha_G L_2}. \tag{121}$$

By separating this last expression into its real and imaginary parts, we get

$$\begin{aligned} &\Theta_2 = \frac{L_1}{L_2}\left[\frac{L_1/L_2 - L_1/F_G + \overline{\Theta}_1}{(L_1/L_2 - L_1/F_G + \overline{\Theta}_1)^2 + (\Lambda_1 + \Omega_G)^2}\right] = 1 + \frac{L_2}{F}, \\ &\Lambda_2 = \frac{L_1}{L_2}\left[\frac{\Lambda_1 + \Omega_G}{(L_1/L_2 - L_1/F_G + \overline{\Theta}_1)^2 + (\Lambda_1 + \Omega_G)^2}\right] = \frac{2L_2}{kW^2}, \\ &\overline{\Theta}_2 = 1 - \Theta_2, \end{aligned} \tag{122}$$

where the finite size of the lens aperture is characterized by the nondimensional Fresnel parameter

$$\Omega_G = \frac{2L_1}{kW_G^2}. \tag{123}$$

Hence, in absence of a random medium, the complex on-axis amplitude of the beam at the output plane can be represented by the product

$$\frac{1}{p(L_1 + L_2)} = (\Theta_1 - i\Lambda_1)(\Theta_2 - i\Lambda_2) = \Theta - i\Lambda, \tag{124}$$

where Θ and Λ are defined by Eqs. (112) and also by

$$\begin{aligned} \Theta &= \Theta_1\Theta_2 - \Lambda_1\Lambda_2, \\ \Lambda &= \Lambda_1\Theta_2 + \Theta_1\Lambda_2. \end{aligned} \tag{125}$$

The parameters Θ_1 and Λ_1 describe beam characteristics of the wave incident on the lens at distance L_1 from the input plane, whereas Θ_2 and Λ_2 describe beam characteristics at the output plane in terms of the propagation distance L_2 from the lens to the output plane. Finally, Θ and Λ describe the complex amplitude at the output plane in terms of the total propagation distance $L = L_1 + L_2$ from the input plane.

The irradiance of the optical wave at the output plane in the absence of turbulence is given by (see Example 2 in Section 4.11)

$$\begin{aligned} I^0(\mathbf{r}, L) = |U_0(\mathbf{r}, L)|^2 &= (\Theta_1^2 + \Lambda_1^2)(\Theta_2^2 + \Lambda_2^2)\exp\left(-2r^2/W^2\right) \\ &= \frac{W_0^2}{W^2(1 + \Omega_G/\Lambda_1)}\exp\left(-\frac{2r^2}{W^2}\right). \end{aligned} \tag{126}$$

The factor $(1 + \Omega_G/\Lambda_1)$ in the denominator of Eq. (126) accounts for power loss of the transmitted beam owing to the finite size of the aperture of the Gaussian lens.

4.9.2 Image plane

The *ABCD* ray-matrix approach described above can be a practical method for certain image plane applications (see Chap. 14). Let F_G denote the focal length of the Gaussian lens in Fig. 4.17 located at distance L_1 from the source. In imaging applications, the distance L_2 from the imaging lens is selected so that $\Theta_2 = 0$, or

$$\frac{L_1}{L_2} - \frac{L_1}{F_G} + \overline{\Theta}_1 = 0. \tag{127}$$

We can interpret (127) as a kind of generalized lens law by noting $\overline{\Theta}_1 = -L_1/F_1$ and then rewriting (127) in the format

$$-\frac{1}{F_1} + \frac{1}{L_2} = \frac{1}{F_G}. \tag{128}$$

For the special case of a point source at the transmitter, we have $F_1 = -L_1$, and therefore (128) reduces to the conventional lens law

$$\frac{1}{L_1} + \frac{1}{L_2} = \frac{1}{F_G}. \tag{129}$$

Imaging systems that permit high spatial frequency content are considered best because high frequencies contain the fine detail of the object being imaged. The frequency analysis of an (incoherent) imaging system can be characterized by the *optical transfer function* (OTF), which is defined as the normalized two-dimensional Fourier transform of the *point spread function* (PSF) which, for a

point source, is the irradiance in the *image plane* of the system. Based on (126), the normalized two-dimensional Fourier transform of the irradiance gives us

$$\frac{\int\int_{-\infty}^{\infty} I^0(\mathbf{r}, L) e^{2\pi i \mathbf{r}\cdot\boldsymbol{\nu}} d^2 r}{\int\int_{-\infty}^{\infty} I^0(\mathbf{r}, L)\, d^2 r} = \exp\left(-\frac{1}{2}\pi^2 \nu^2 W^2\right), \tag{130}$$

where ν is the magnitude of the spatial frequency. In the particular case of a point source that is far from the imaging lens, we have $\Lambda_2 = L_1/L_2\Omega_G$ and $L_2 \cong F_G$. Hence, the image plane spot size is approximately $W = \lambda F_G/\pi W_G$. It is customary to relate the "soft-aperture" spot radius of the Gaussian lens to the actual "hard-aperture" diameter D_G of the lens by $D_G^2 = 8W_G^2$. Under this condition, the Gaussian approximation for the OTF [deduced from Eq. (130)] becomes

$$\mathrm{OTF}_0(\nu) = \exp\left[-4\left(\frac{\lambda F_G \nu}{D_G}\right)^2\right]. \tag{131}$$

In general, the OTF is a complex quantity and the *magnitude* of the OTF is called the *modulation transfer function* (MTF), viz., $\mathrm{MTF}_0(\nu) = |\mathrm{OTF}_0(\nu)|$. Clearly then, because Eq. (131) is real, it also represents the MTF in this case so we have

$$\mathrm{MTF}_0(\nu) = |\mathrm{OTF}_0(\nu)| = \exp\left[-4\left(\frac{\lambda F_G \nu}{D_G}\right)^2\right]. \tag{132}$$

For a hard-aperture lens system, it is well known that the MTF is described by [20]

$$\mathrm{MTF}_0(\nu) = \begin{cases} \dfrac{2}{\pi}\left[\cos^{-1}(\lambda F_G \nu/D_G) - (\lambda F_G \nu/D_G)\sqrt{1-(\lambda F_G \nu/D_G)^2}\right], & \nu \le D_G/\lambda F_G, \\ 0, & \nu > D_G/\lambda F_G, \end{cases} \tag{133}$$

which limits the spatial frequencies of the system to $\nu \le D_G/\lambda F_G$. Note that the actual cutoff spatial frequency $\nu = D_G/\lambda F_G$ in (133) corresponds to the value of the MTF (132) given by $e^{-4} \approx 0.018$. For the purpose of comparison, the graphs of MTFs defined by Eqs. (132) and (133), as a function of $\lambda F_G \nu/D_G$, are illustrated in Fig. 4.18.

One measure of the resolution achieved by an imaging system is defined by the volume lying under the MTF surface. Based on either (132) or (133), this definition of *resolution* leads to the same result

$$R = \int_0^{2\pi}\int_0^{\infty} \nu \mathrm{MTF}_0(\nu)\, d\nu\, d\theta = \frac{\pi D_G^2}{4\lambda^2 F_G^2}. \tag{134}$$

From this expression it is clear that resolution (imaging) in free space improves with an increase in the size of the lens. This is not necessarily the case in turbulence.

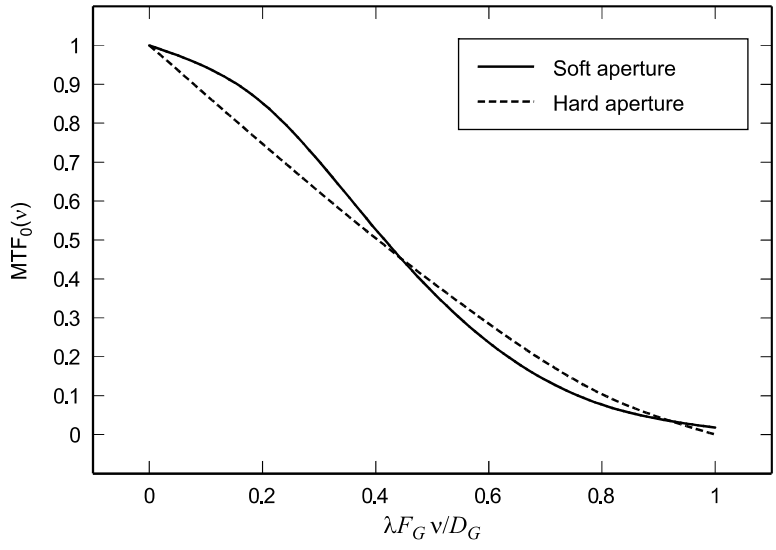

Figure 4.18 MTF for a lens of diameter D_G and focal length F_G. The solid curve depicts the "soft-aperture" Gaussian approximation (132) and the dashed curve is the "hard-aperture" exact result (133).

4.9.3 Gaussian mirror

The double passage of an optical wave over the same propagation path in the presence of a random medium is of great interest in the analysis of laser radar systems (see Chap. 13). Double passage propagation occurs if, after propagating a distance L, the optical wave is incident on a target that sends the wave back in the original direction to a receiver colocated with the transmitter. In this case the total propagation path length is $2L$ and the configuration is called a *monostatic channel*. If the target is a smooth reflector (*mirror*) with finite size and focal length, its *ABCD* representation is essentially the same as that of a thin Gaussian lens; hence, such a target can be referred to as a *Gaussian mirror*.

For the case of a wave reflected from a smooth surface, let $L_1 = L_2 = L$ in Fig. 4.17 for a total propagation distance $2L$ and replace the Gaussian lens by a Gaussian mirror with effective radius W_R and focal length F_R. The resulting configuration in Fig. 4.17 is then equivalent to a double-pass or folded-path system with the path unfolded. Finally, the beam parameters of the reflected wave back in the plane of the transmitter/receiver (transceiver) are described by

$$\begin{aligned} \Theta_2 &= \frac{2 - \Theta_1 - L/F_R}{(2 - \Theta_1 - L/F_R)^2 + (\Lambda_1 + \Omega_R)^2}, \\ \Lambda_2 &= \frac{\Lambda_1 + \Omega_R}{(2 - \Theta_1 - L/F_R)^2 + (\Lambda_1 + \Omega_R)^2}, \end{aligned} \tag{135}$$

where $\Omega_R = 2L/kW_R^2$.

Note that the reflected wave described by (135) is a focused beam provided the focal length of the mirror is chosen so that $L/F_R = 2 - \Theta_1$. For a transmitted plane wave ($\Theta_1 = 1, \Lambda_1 = 0$), this requires $L/F_R = 1$ (the receiver is in the focal plane), whereas for a spherical wave ($\Theta_1 = \Lambda_1 = 0$) it leads to $L/F_R = 2$ (the receiver is in the plane defined by the radius of curvature of the mirror).

4.10 Summary and Discussion

In this chapter we discussed the diffractive properties of a TEM_{00} Gaussian-beam wave propagating in free space. For our applications it is sufficient to describe these properties using a *scalar theory* and the *paraxial approximation.* The basic beam characteristics at the transmitter ($z = 0$) are its

- *wave number* $k = 2\pi/\lambda$ (where λ is *wavelength*)
- *spot size radius* W_0
- *phase front radius of curvature* F_0

For a beam that has propagated a distance z from the transmitter (input plane), these characteristics are used to define a set of *input plane beam parameters*

$$\text{Input Plane:} \quad \Theta_0 = 1 - \frac{z}{F_0}, \quad \Lambda_0 = \frac{2z}{kW_0^2} \tag{136}$$

We designate the type of beam by the following:

- *collimated beam*: $\Theta_0 = 1$
- *convergent beam*: $\Theta_0 < 1$
- *divergent beam*: $\Theta_0 > 0$

The field of an optical wave at a receiver placed distance z from the source can be obtained from the *Huygens-Fresnel integral*

$$\begin{aligned} U_0(\mathbf{r}, z) &= -\frac{ik}{2\pi z}\exp(ikz)\int\int_{-\infty}^{\infty} U_0(\mathbf{s}, 0)\exp\left(\frac{ik}{2z}|\mathbf{s}-\mathbf{r}|^2\right)d^2s \\ &= \frac{1}{\Theta_0 + i\Lambda_0}\exp(ikz)\exp\left(-\frac{r^2}{W^2} - i\frac{kr^2}{2F}\right), \end{aligned} \tag{137}$$

where $U_0(\mathbf{s}, 0)$ is the Gaussian-beam wave at the emitting aperture of the source. Equation (137) shows that the wave at the receiver is also a Gaussian beam with new spot size W and phase front radius of curvature F. The quantity $1/(\Theta_0 + i\Lambda_0) = \Theta - i\Lambda$ is the *complex amplitude* of the received wave and $\exp(ikz)$ introduces an unimportant phase term associated with the plane-wave aspect of the beam.

In the plane of the receiver, we define the *output plane beam parameters*:

$$\text{Output Plane:} \quad \begin{aligned} \Theta &= \frac{\Theta_0}{\Theta_0^2 + \Lambda_0^2} = 1 + \frac{z}{F} \\ \overline{\Theta} &= 1 - \Theta \\ \Lambda &= \frac{\Lambda_0}{\Theta_0^2 + \Lambda_0^2} = \frac{2z}{kW^2} \end{aligned} \tag{138}$$

With either input plane or output plane beam parameters, the *beam spot radius, phase front radius of curvature*, and *mean irradiance* (*intensity*) at the receiver are defined by:

$$\text{Spot Radius:} \quad W = W_0\sqrt{\Theta_0^2 + \Lambda_0^2} = \frac{W_0}{\sqrt{\Theta^2 + \Lambda^2}} \tag{139}$$

$$\text{Radius of Curvature:} \quad \begin{aligned} F &= \frac{F_0\left(\Theta_0^2 + \Lambda_0^2\right)(\Theta_0 - 1)}{\Theta_0^2 + \Lambda_0^2 - \Theta_0} \\ F &= \frac{F_0\left(\Theta^2 + \Lambda^2 - \Theta\right)}{(\Theta - 1)\left(\Theta^2 + \Lambda^2\right)} \end{aligned} \tag{140}$$

$$\text{Mean Irradiance:} \quad \begin{aligned} I^0(r, L) &= \frac{1}{\Theta_0^2 + \Lambda_0^2}\exp(-2r^2/W^2) \\ I^0(r, L) &= (\Theta^2 + \Lambda^2)\exp(-2r^2/W^2) \end{aligned} \tag{141}$$

Additional parameters developed here for a propagating beam include the following:

$$\textit{Focusing parameter}: \quad \Omega_f = \frac{2F_0}{kW_0^2} \tag{142}$$

$$\textit{Spot size radius at beam waist}: \quad W_B = \frac{W_0|\Omega_f|}{\sqrt{1 + \Omega_f^2}} = \frac{2F_0}{kW_0\sqrt{1 + \Omega_f^2}} \tag{143}$$

$$\textit{Spot size radius at geometric focus}: \quad W_f = W_0\Omega_f = \frac{2F_0}{kW_0} \tag{144}$$

The higher-order Hermite-Gaussian (HG) and Laguerre-Gaussian (LG) modes (TEM_{mn}) of a collimated beam were also briefly discussed. For the HG beams it is customary to describe a TEM_{00} spot size along each transverse coordinate axis. Except for the TEM_{00} mode, the distinguishing characteristic of higher-order HG or LG waves is the irradiance consists of a pattern of spots (e.g., recall Fig. 4.9) rather than a single spot. In the plane of the receiver, the effective spot size of the beam can be defined by the rectangular domain $\sigma_{x,m}(z) \times \sigma_{y,n}(z)$, where

$$\begin{aligned} &\text{Hermite Gaussian} \quad \sigma_{x,m}(z) = \sqrt{2m+1}W_x(z), \quad m = 0, 1, 2, \ldots, \\ &\text{Spot Size:} \quad \sigma_{y,n}(z) = \sqrt{2n+1}W_y(z), \quad n = 0, 1, 2, \ldots, \end{aligned} \tag{145}$$

and where W_x and W_y represent spot radii in the x and y directions, respectively, associated with the TEM_{00} mode. In the case of the LG beams, the comparable expression for the spot size is given by

$$\text{Laguerre-Gaussian Spot Size:} \quad \sigma_{mn}(z) = \sqrt{2n+m+1}W(z); \quad m, n = 0, 1, 2, \ldots. \tag{146}$$

Last, we discussed the use of *ABCD* ray matrices to characterize the propagation path between input and output planes when one or more optical elements (lenses, aperture stops, etc.) are located along the optical axis and perfectly aligned. This formulation permits us to identify the total propagation path by a single *ABCD* matrix obtained from the cascade scheme of (left-hand) multiplication of successive matrix representations for each optical element and straight line segment between elements. The validity of the paraxial approximation used in this approach is based on the idea that the distance between optical elements is much greater than the transverse dimension of the optical wave. And, although here we only considered systems that are rotationally symmetric, the *ABCD* matrix approach is equally valid in rectangular coordinates [4].

In an *ABCD* optical system, the field of the optical wave at the output plane deduced from the *generalized Huygens-Fresnel integral* is

$$\begin{aligned} U_0(\mathbf{r}, L) &= -\frac{ik}{2\pi B}\exp(ikL)\int\int_{-\infty}^{\infty} d^2s \exp\left(-\frac{1}{2}\alpha_0 k s^2\right)\exp\left[\frac{ik}{2B}\left(As^2 - 2\mathbf{s}\cdot\mathbf{r} + Dr^2\right)\right] \\ &= \frac{1}{A + i\alpha_0 B}\exp(ikL)\exp\left[-\frac{1}{2}\left(\frac{\alpha_0 D - iC}{A + i\alpha_0 B}\right)kr^2\right], \end{aligned} \tag{147}$$

where *A, B, C*, and *D* are the ray-matrix elements that characterize the overall propagation path between input and output planes.

To further facilitate the description of Gaussian-beam waves through a such a train of optical elements, particularly in the presence of optical turbulence (see Chap. 10), we find it is useful to characterize the Gaussian-beam wave incident on each optical element by a pair of beam parameters similar to the

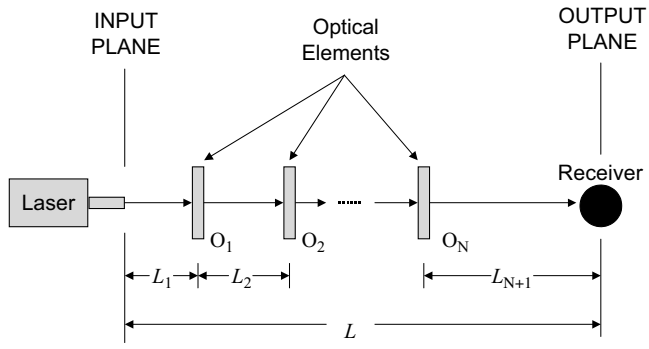

Figure 4.19 Schematic representation of optical wave propagation through a general propagation system consisting of a train of optical elements $O_1, O_2, \ldots, O_N$ arbitrarily located (but perfectly aligned) along the propagation path.

output beam parameters for a simple line-of-sight path. This will necessitate the introduction of several pairs of beam parameters when several optical elements exist along the path, each of which is related to the previous pair of beam parameters by a simple conformal mapping using a reciprocal transformation of the form $Z = C/\zeta$, where Z and ζ represent two complex planes and C is a real constant. The (on-axis) complex amplitude associated with such a system consisting on N optical elements and $N+1$ straight line segments can then be expressed in the product form (see Fig. 4.19)

$$\frac{1}{p(L)} = \prod_{m=1}^{N+1} (\Theta_m - i\Lambda_m) = \Theta - i\Lambda, \tag{148}$$

where $L = L_1 + L_2 + \cdots + L_{N+1}$.

For example, in the special case of a single "Gaussian lens" (i.e., a thin lens and a finite aperture stop) at distance L_1 from the transmitter, we introduce *three sets* of beam parameters defined, respectively, by

$$z = 0: \quad \Theta_0 = 1 - \frac{L_1}{F_0}, \quad \Lambda_0 = \frac{2L_1}{kW_0^2} \tag{149}$$

$$\begin{aligned} z = L_1: \quad \Theta_1 &= \frac{\Theta_0}{\Theta_0^2 + \Lambda_0^2} = 1 + \frac{L_1}{F_1} \\ \overline{\Theta}_1 &= 1 - \Theta \\ \Lambda_1 &= \frac{\Lambda_0}{\Theta_0^2 + \Lambda_0^2} = \frac{2L_1}{kW_1^2} \end{aligned} \tag{150}$$

$$
\begin{aligned}
z = L_1 + L_2: \quad \Theta_2 &= \frac{L_1}{L_2}\left[\frac{L_1/L_2 - L_1/F_G + \overline{\Theta}_1}{(L_1/L_2 - L_1/F_G + \overline{\Theta}_1)^2 + (\Lambda_1 + \Omega_G)^2}\right] = 1 + \frac{L_2}{F} \\
\overline{\Theta}_2 &= 1 - \Theta_2 \\
\Lambda_2 &= \frac{L_1}{L_2}\left[\frac{\Lambda_1 + \Omega_G}{(L_1/L_2 - L_1/F_G + \overline{\Theta}_1)^2 + (\Lambda_1 + \Omega_G)^2}\right] = \frac{2L_2}{kW^2}
\end{aligned}
\tag{151}
$$

Here the thin lens has focal length F_G and Gaussian limiting aperture radius W_G, and $\Omega_G = 2L_1/kW_G^2$ is a nondimensional parameter that characterizes the finite size of the lens. The irradiance at the output plane ($z = L_1 + L_2 = L$) obtained from (147) is

$$
\begin{aligned}
I^0(\mathbf{r}, L) &= \frac{1}{|A + i\alpha_0 B|^2}\exp\left[-\mathrm{Re}\left(\frac{\alpha_0 D - iC}{A + i\alpha_0 B}\right)kr^2\right] \\
&= (\Theta_1^2 + \Lambda_1^2)(\Theta_2^2 + \Lambda_2^2)\exp\left(-\frac{2r^2}{W^2}\right) \\
&= \frac{W_0^2}{W^2(1 + \Omega_G/\Lambda_1)}\exp\left(-\frac{2r^2}{W^2}\right)
\end{aligned}
\tag{152}
$$

Last, the above beam parameters are also valid for the case when the Gaussian lens is replaced by a Gaussian mirror that reflects the wave back to the input plane, with $L_1 = L_2 = L$ so the total propagation path in this case is taken as $2L$ (see Chap. 13).

4.11 Worked Examples

Example 1: Assume the initial beam characteristics of a unit amplitude Gaussian beam at the transmitter are given by

$$
\begin{aligned}
W_0 &= 0.03\,\mathrm{m}, \\
F_0 &= 500\,\mathrm{m}, \\
\lambda &= 0.633\,\mu\mathrm{m}.
\end{aligned}
$$

For a receiver at distance $z = L = 1200\,\mathrm{m}$ from the transmitter, calculate the following beam characteristics along the propagation path:

(*a*) spot radius at the receiver
(*b*) radius of curvature at the receiver
(*c*) on-axis mean irradiance at the receiver
(*d*) propagation distance to beam waist
(*e*) beam radius at the waist
(*f*) beam radius at the geometric focus

Solution: We first calculate beam parameters:

$$\Theta_0 = 1 - \frac{L}{F_0} = -1.4, \quad \Lambda_0 = \frac{2L}{kW_0^2} = 0.2687.$$

(*a*) $W = W_0\sqrt{\Theta_0^2 + \Lambda_0^2} = 4.3\,\text{cm}$

(*b*) $F = \dfrac{F_0(\Theta_0^2 + \Lambda_0^2)(\Theta_0 - 1)}{(\Theta_0^2 + \Lambda_0^2 - \Theta_0)} = -710.5\,\text{m}$

(*c*) $I(0, L) = \dfrac{W_0^2}{W^2} = 0.492\,\text{W/m}^2$

(*d*) $z_B = \dfrac{F_0}{1 + \Omega_f^2} = 494\,\text{m}$

(*e*) $W_B = W_0\sqrt{\dfrac{\Omega_f^2}{1 + \Omega_f^2}} = 0.33\,\text{cm}$

(*f*) $W_f = \dfrac{2F_0}{kW_0} = 0.34\,\text{cm}$

❑

Example 2: Derive the expression for the on-axis irradiance given in Eq. (126).

Solution: From Eq. (124), we see that the on-axis irradiance is

$$I^0(0, L) = \frac{1}{|p(L)|^2} = (\Theta_1^2 + \Lambda_1^2)(\Theta_2^2 + \Lambda_2^2).$$

The spot radius W_1 of the optical wave incident on the Gaussian lens and the spot radius V_1 of the optical wave emerging from the lens are related by a kind of lens law

$$\frac{1}{V_1^2} = \frac{1}{W_1^2} + \frac{1}{W_G^2},$$

where W_G is the spot radius of the lens. Thus, it follows that

$$V_1^2 = W_1^2(1 + W_1^2/W_G^2)^{-1} = W_1^2(1 + \Omega_G/\Lambda_1)^{-1}$$

and

$$\Theta_1^2 + \Lambda_1^2 = \frac{W_0^2}{W_1^2},$$

$$\Theta_2^2 + \Lambda_2^2 = \frac{V_1^2}{W^2} = \frac{W_1^2}{W^2(1 + \Omega_G/\Lambda_1)}.$$

Consequently, the on-axis irradiance takes the form

$$I^0(0,L) = (\Theta_1^2 + \Lambda_1^2)(\Theta_2^2 + \Lambda_2^2) = \frac{W_0^2}{W^2(1 + \Omega_G/\Lambda_1)}.$$

❑

Example 3: Consider a unit amplitude Gaussian beam at the transmitter described by the following parameters:

$$W_0 = 0.05\,\text{m},$$
$$F_0 = 500\,\text{m},$$
$$\lambda = 0.633\,\mu\text{m}.$$

Assume that a thin Gaussian lens with $W_G = 4$ cm and $F_G = 5$ cm is placed at the end of the path $L_1 = 1200$ m. If the signal is detected at distance $L_2 = 1$ m behind the lens, calculate at this point:

(*a*) the spot radius
(*b*) the radius of curvature
(*c*) the mean on-axis intensity

Solution: To begin, we make the following calculations:

$$\Theta_0 = 1 - \frac{L_1}{F_0} = -\frac{7}{5}, \quad \Lambda_0 = \frac{2L_1}{kW_0^2} = 0.0967,$$

$$\Theta_1 = \frac{\Theta_0}{\Theta_0^2 + \Lambda_0^2} = -0.7109, \quad \Lambda_1 = \frac{\Lambda_0}{\Theta_0^2 + \Lambda_0^2} = 0.0491, \quad \Omega_G = \frac{2L_1}{kW_G^2} = 0.1511,$$

$$\Theta_2 = \frac{L_1}{L_2}\left[\frac{L_1/L_2 - L_1/F_G + 1 - \Theta_1}{(L_1/L_2 - L_1/F_G + 1 - \Theta_1)^2 + (\Lambda_1 + \Omega_G)^2}\right] = -0.0526,$$

$$\Lambda_2 = \frac{L_1}{L_2}\left[\frac{\Lambda_1 + \Omega_G}{(L_1/L_2 - L_1/F_G + 1 - \Theta_1)^2 + (\Lambda_1 + \Omega_G)^2}\right] = 4.62 \times 10^{-7}.$$

Based on these results, we then obtain

(*a*) $W = \sqrt{\dfrac{2L_2}{k\Lambda_2}} = 66\,\text{cm}$

(*b*) $F = L_2/(\Theta_2 - 1) = -95\,\text{cm}$

(*c*) $I^0(0,L) = 0.0014\,\text{W/m}^2$

❑

Example 4: Solve the following initial value problem [recall (27)] and thus deduce the Huygens-Fresnel integral (25):

$$\frac{1}{r}\frac{\partial}{\partial r}\left(r\frac{\partial V}{\partial r}\right) + 2ik\frac{\partial V}{\partial z} = 0,$$
$$V(r,0) \equiv U_0(r,0) = \exp\left(-\frac{r^2}{W_0^2} - \frac{ikr^2}{2F_0}\right).$$

Solution: Because this is an initial value problem, we will transform the problem by applying the Laplace transform relations

$$\mathscr{L}\{V(r,z); z \to p\} = \int_0^\infty e^{-pz}V(r,z)\,dz = \hat{V}(r,p), \quad p > 0,$$
$$\mathscr{L}\left\{\frac{\partial V}{\partial z}; z \to p\right\} = p\hat{V}(r,p) - U_0(r,0),$$
$$\mathscr{L}\left\{\frac{1}{r}\frac{\partial}{\partial r}\left(r\frac{\partial V}{\partial r}\right);\ z \to p\right\} = \frac{1}{r}\frac{\partial}{\partial r}\left(r\frac{\partial \hat{V}}{\partial r}\right),$$

which lead to the transformed equation

$$\frac{1}{r}\frac{\partial}{\partial r}\left(r\frac{\partial \hat{V}}{\partial r}\right) + 2ikp\hat{V} = 2ikU_0(r,0).$$

The two-dimensional free-space Green's function for the Helmholtz operator in the above equation is

$$\hat{g}(\mathbf{s},\mathbf{r};p) = \frac{i}{4}H_0^{(1)}\left(\sqrt{2ikp}|\mathbf{s}-\mathbf{r}|\right) = \frac{1}{2\pi}K_0\left(\sqrt{-2ikp}|\mathbf{s}-\mathbf{r}|\right),$$

where $H_0^{(1)}(x) = J_0(x) + iY_0(x)$ is the *Hankel function of the first kind* expressed in terms of standard Bessel functions and $K_0(x)$ is the *modified Bessel function of the second kind.* Hence, we can write

$$\hat{V}(r,p) = -2ik\int\int_{-\infty}^{\infty}\hat{g}(\mathbf{s},\mathbf{r};p)U_0(\mathbf{s},0)\,d^2s.$$

At this point, we apply the inverse Laplace transform to both sides, interchange the order of integration, and multiply the result by e^{ikz} to find

$$U_0(r,z) = -2ike^{ikz}\int\int_{-\infty}^{\infty}g(\mathbf{s},\mathbf{r};z)U_0(\mathbf{s},0)\,d^2s$$
$$= -2ik\int\int_{-\infty}^{\infty}G(\mathbf{s},\mathbf{r};z)U_0(\mathbf{s},0)\,d^2s,$$

where $G(\mathbf{s},\mathbf{r};z) = e^{ikz}g(\mathbf{s},\mathbf{r};z)$ and

$$g(\mathbf{s},\mathbf{r};z) = \mathscr{L}^{-1}\{\hat{g}(\mathbf{s},\mathbf{r};p);p\to z\} = \frac{1}{2\pi}\mathscr{L}^{-1}\left\{K_0^{(1)}\left(\sqrt{-2ikp}|\mathbf{s}-\mathbf{r}|\right);p\to z\right\}$$
$$= \frac{1}{4\pi z}\exp\left[\frac{ik}{2z}|\mathbf{s}-\mathbf{r}|^2\right].$$

Problems

Section 4.2

1. Show that the substitution $U_0(r,z) = V(r,z)e^{ikz}$ into the reduced wave equation (4) leads to

$$\frac{1}{r}\frac{\partial}{\partial r}\left(r\frac{\partial V}{\partial r}\right) + \frac{\partial^2 V}{\partial z^2} + 2ik\frac{\partial V}{\partial z} = 0.$$

Section 4.3

2. Verify that the plane wave solution (11) satisfies the paraxial equation (9).
3. Verify that the spherical wave solution (13) satisfies the paraxial equation (9).
4. Under the assumption

$$V(r,z) = A(z)\exp\left[-\frac{1}{p(z)}\left(\frac{\alpha_0 k r^2}{2}\right)\right]$$

show that the paraxial equation (9) simplifies to

$$\alpha_0^2 k^2 r^2 A(z) + i\alpha_0 k^2 r^2 A(z)p'(z) - 2\alpha_0\, kA(z)p(z) + 2ikA'(z)p^2(z) = 0.$$

5. Use separation of variables to show that the solution of the differential equation in (22) is given by $A(z) = 1/p(z)$.

Section 4.4

6. From (44) and the relations $\Lambda = 2L/kW^2$ and $\Theta = 1 + L/F$,
   (*a*) Deduce that the spot size and phase front radius of curvature at the receiver are given by

$$W = W_0\sqrt{\Theta_0^2 + \Lambda_0^2}, \quad F = \frac{F_0(\Theta_0^2 + \Lambda_0^2)(\Theta_0 - 1)}{\Theta_0^2 + \Lambda_0^2 - \Theta_0}.$$

   (*b*) Deduce from (*a*) that, for a collimated beam, the phase front radius of curvature reduces to

$$F = -z\left(1 + \frac{1}{\Lambda_0^2}\right).$$

7. From Eqs. (37), (38), and (44), deduce the following relations:

$$(a)\quad W = \frac{W_0}{\sqrt{\Theta^2 + \Lambda^2}}. \qquad (b)\quad F = \frac{F_0(\Theta^2 + \Lambda^2 - \Theta)}{(\Theta - 1)(\Theta^2 + \Lambda^2)}.$$

8. A collimated beam with $\lambda = 0.5\,\mu\text{m}$ and $W_0 = 1\,\text{cm}$ is transmitted to a receiver located 1 km downrange from the transmitter.
   (*a*) Determine the beam receiver parameters Θ and Λ.
   (*b*) What is the spot size and the phase front radius of curvature at the receiver?

9. A collimated beam with $\lambda = 0.5\,\mu\text{m}$ has a spot size $W = 7\,\text{cm}$ at distance 10 km from the transmitter. What is the spot size W_0 at the transmitter?

10. For a propagating Gaussian beam at distance z from the transmitter, show that the spot size and phase front radius of curvature satisfy the relation $\partial W/\partial z = -W/F$.

11. For a collimated beam over a fixed path length L,
   (*a*) show that $\Lambda_{\max} = 1/2$ and, further, that $0 \le \Lambda \le 1/2, 0 \le \Theta \le 1$.
   (*b*) show that the beam of minimum spot size at the receiver corresponds to $\Lambda_0 = 1$.

Section 4.5

12. By minimizing the beam spot size given in Prob. 6 with respect to propagation distance z, deduce that the distance to the beam waist and beam waist spot size are, respectively, given by

$$z_B = \frac{F_0}{1+\Omega_f^2}, \quad W_B = \frac{W_0|\Omega_f|}{\sqrt{1+\Omega_f^2}}.$$

13. A convergent beam with $\lambda = 0.5\mu\text{m}$ and spot size 5 cm at the transmitter is observed at distance 500 m from the transmitter with spot size 2 cm. Identify the position of the beam waist if it is
   (*a*) located somewhere between the transmitter and receiver.
   (*b*) located somewhere beyond the receiver.

14. Prove that $\Omega_f = 1$ places the beam waist at maximum distance from the transmitter.

15. A beam focused at 1000 m with $\lambda = 0.5\mu\text{m}$ has a spot *diameter* at 5 km of 17.8 cm.
   (*a*) What is the spot *diameter* (in cm) at the transmitter aperture?
   (*b*) What is the phase front radius of curvature of this beam at 5 km?
   (*c*) If the same size beam at the transmitter is now focused at 5 km, what is the spot size diameter and phase front radius of curvature at 5 km?
   (*d*) Under the conditions in (*c*), what is the beam diameter (in cm) at the *beam waist* and at what distance from the transmitter is the waist located?

16. Derive Eqs. (61) for the location of the Rayleigh range and show that these positions correspond to points P_1 and P_2 shown in Fig. 4.6.

17. Show that the Rayleigh range for a collimated beam is given by $0 \leq \Lambda_0 \leq 1$.

18. Treating the spot size W as a function of focal length F_0, show that to place *maximum energy* on a target at fixed distance L from the transmitting aperture the beam should be focused on the target (i.e., $F_0 = L$).
Hint: Minimize the spot size.

Section 4.6

19. For Example 1 in the Worked examples section, calculate the Rayleigh range.
Ans. $439 < z < 549$ m.

20. Under the conformal mapping (62), show that the ray-line (54) in the p-plane becomes the circle (63) in the complex amplitude plane.

21. Show that, given the spot size W_0 at the input plane and the spot size W at the output plane ($z = L$), the size and location of the beam waist is given by

$$W_B = \frac{2L/kW_0}{\sqrt{1 + W^2/W_0^2 - 2\Theta_0}}, \quad z_B = \frac{L(1 - \Theta_0)}{1 + W^2/W_0^2 - 2\Theta_0}.$$

Section 4.7

22. Use (82) to evaluate the integrals in (81) and deduce that the effective x and y spot sizes of the Hermite-Gaussian beam are given by Eqs. (83).

23. Prove that the spot size $\sigma_{x,m}(z)$ from (83) contains all irradiance maxima of the Hermite polynomial $H_m(\sqrt{2}x/W_x)$.

24. *Elegant Hermite polynomials* [4].
(*a*) Show that $q(z) = [2p(z)/k\alpha]^{1/2}$ is a solution of Eq. (72).
(*b*) For the choice of $q(z)$ given in (*a*), show that the solution of Eq. (73) is

$$A(z) = \frac{1}{(\Theta_0 + i\Lambda_0)^{(m+1)/2}}.$$

(*c*) Finally, by assuming the spot size in the x direction is the same as that in the y direction, show that

$$V_{mn}(x, y, z) = (\Theta - i\Lambda)^{(m+n+2)/2} H_m\left(x\sqrt{b}\right) H_n\left(y\sqrt{b}\right) \times \exp[-b(x^2 + y^2)] \exp\left[-\frac{i}{2}(m + n + 2)\tan^{-1}\frac{\Lambda}{\Theta}\right],$$

where $b = -(ik/2z)(\overline{\Theta} + i\Lambda)$.

25. Assume the higher-order modes of a collimated beam at the exit aperture of a laser are described by

$$U_{mn}(x,y,0) = H_m\left(\frac{\sqrt{2}x}{W_0}\right) H_n\left(\frac{\sqrt{2}y}{W_0}\right) \exp\left(-\frac{x^2+y^2}{W_0^2}\right),$$

where $W = W_0\sqrt{1+\Lambda_0^2} = W_0/\sqrt{\Theta^2+\Lambda^2}$. Use the Huygens-Fresnel integral (84) to derive Eq. (86).

Hint: $\displaystyle\int_{-\infty}^{\infty} H_n(ax)e^{-(x-y)^2}dx = \sqrt{\pi}(1-a^2)^{n/2}H_n\left(\frac{ay}{\sqrt{1-a^2}}\right)$.

26. Use a relation analogous to (81) to deduce that the effective spot size of a Laguerre-Gaussian beam is that given by (90).

Section 4.8

27. If the Gaussian-beam wave at the emitting aperture of a laser transmitter is

$$U_0(\mathbf{r},0) = \exp\left(-\frac{1}{2}\alpha_0 kr^2\right),$$

use the generalized Huygens-Fresnel integral (107) to deduce that the Gaussian-beam wave at the receiver ($z = L$), after passing through an optical system characterized by an *ABCD* ray matrix, is given by

$$U_0(\mathbf{r},L) = \frac{1}{A+i\alpha_0 B}\exp(ikL)\exp\left[-\frac{1}{2}\left(\frac{\alpha_0 D - iC}{A+i\alpha_0 B}\right)kr^2\right].$$

28. Use the result of Prob. 27 for the field of an optical wave in the receiver plane of an *ABCD* optical system with all real matrix elements (no aperture stops) to find an expression for (not involving i)
    (*a*) the spot radius W in the plane of the receiver in terms of the matrix elements *A, B, C*, and *D*, given that

$$\frac{2}{kW^2} = \mathrm{Re}\left(\frac{\alpha_0 D - iC}{A+i\alpha_0 B}\right).$$

    (*b*) the phase front radius of curvature in the plane of the receiver in terms of the matrix elements *A, B, C*, and *D*, given that

$$\frac{1}{F} = \mathrm{Im}\left(\frac{\alpha_0 D - iC}{A+i\alpha_0 B}\right).$$

    (*c*) For line-of-sight propagation (no optical elements along the path), show that the answers in parts (*a*) and *(b)* reduce to the results of Eqs. (37) and (38).

Section 4.9

29. If a thin lens with focal length f is placed at the input plane and the beam propagates to a receiver at distance L beyond the lens,
    (*a*) determine the overall *ABCD* matrix for the optical channel.
    (*b*) If the beam incident on the thin lens is a collimated beam with spot size W_0, what is the spot size of the beam wave at the receiver?
    (*c*) What is the phase front radius of curvature at the receiver for the collimated beam in part (*b*)?

30. If the thin lens in Prob. 29 is placed at the output plane in front of the receiver,
    (*a*) determine the overall *ABCD* matrix for the optical channel.
    (*b*) If the beam at the input plane is a collimated beam with spot size W_0, what is the spot size of the beam wave at the receiver?
    (*c*) What is the phase front radius of curvature at the receiver for the collimated beam in part (*b*)?

31. Solve Prob. 29 if the lens is replaced by a limiting aperture of effective radius σ.

32. Solve Prob. 30 if the lens is replaced by a limiting aperture of effective radius σ.

33. Two lenses along the propagation path of an optical wave are separated by distance $f_1 + f_2$, where f_1 is the focal length of the first lens and f_2 is the focal length of the second lens (see figure).

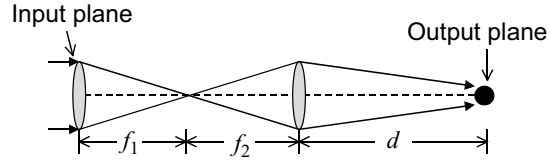

    (*a*) If the first lens is at the input plane and the optical wave propagates a distance d after passing through the second lens, what is the *ABCD* ray matrix for the optical system?
    (*b*) At what distance d will the matrix element $B = 0$?
    (*c*) For a collimated beam of radius W_0 incident on the first lens, determine $p(L)$ and $\alpha(L)$ given that $L = f_1 + f_2 + d$, where d satisfies the condition of part (*b*).

34. Consider a unit amplitude collimated beam located at the front focal plane of a large (infinite) lens with focal length $f > 0$.
    (*a*) Find the Gaussian-beam wave at the back focal plane of the lens at $z = 2f$.
    (*b*) Show that the answer in part (*a*) is the two-dimensional Fourier transform of the given collimated beam (to within a phase factor).

35. If the input/output planes of an imaging system satisfy Eq. (127),
    (*a*) What is the optical field at the output plane given the general Gaussian-beam wave (108) at the input plane?
    (*b*) Determine the spot radius and phase front radius of curvature.

36. Consider the geometry in which the Gaussian lens in Fig. 4.17 is located midway between input and output planes, i.e., $L_1 = L_2 = L$. For an incident spherical wave, show that the wave emerging from the lens is a Gaussian-beam wave with beam radius $W_0 = W_G$ and phase front radius of curvature $F_0 = 1/F_G - 1/L$, where W_G and F_G denote the finite aperture radius and focal length, respectively, of the lens.

References

1. V. I. Tatarskii, *Wave Propagation in a Turbulent Medium* (McGraw-Hill, New York, 1961), trans. by R. A. Silverman.
2. A. Ishimaru, *Wave Propagation and Scattering in Random Media* (IEEE Press, Piscataway, New Jersey, 1997); [previously published as Vols I & II by Academic, New York (1978)].
3. H. W. Kogelnik and T. Li, "Laser beams and resonators," *Appl. Opt.* **5**, 1550–1567 (1966).
4. A. Siegman, *Lasers* (University Science, Mill Valley, Calif., 1986).
5. J. W. Goodman, *Introduction to Fourier Optics* (McGraw-Hill, New York, 1968).
6. L. C. Andrews, *Special Functions of Mathematics for Engineers*, 2nd ed. (SPIE Optical Engineering Press, Bellingham, Wash.; Oxford University Press, Oxford, 1998); [formerly published as 2nd ed. by McGraw-Hill, New York (1992)].
7. E. Delano, "First order design and the $y\bar{y}$ diagram," *Appl. Opt.* **2**, 1251–125 (1963).
8. S. A. Collins, "Analysis of optical resonators involving focusing elements," *Appl. Opt.* **3**, 1263–1275 (1964).
9. T. Li, "Dual forms of the Gaussian beam chart," *Appl. Opt.* **3**, 1315–1317 (1964).
10. H. W. Kolgelnik, "On the propagation of Gaussian beams of light through lenslike media including those with a loss or gain variation," *Appl. Opt.* **4**, 1562–1569 (1965).
11. J. A. Arnaud, "Degenerate optical cavities," *Appl. Opt.* **8**, 189–195 (1969).
12. S. A. Collins "Lens-system diffraction integral written in terms of matrix optics," *J. Opt. Soc. Am.* **60**, 1168–1177 (1970).
13. J. A. Arnaud, "Representation of Gaussian beams by complex rays," *Appl. Opt.* **24**, 538–543 (1985).
14. D. Kessler and R. V. Schack, "$y\bar{y}$ diagram, a powerful optical design method for laser systems," *Appl. Opt.* **31**, 2692–2707 (1992).
15. L. C. Andrews, W. B. Miller, and J. C. Ricklin, "Geometrical representation of Gaussian beams propagating through complex paraxial optical systems," *Appl. Opt.* **32**, 5918–5929 (1993).
16. R. V. Churchille and J. W. Brown, *Complex Variables and Applications*, 5th ed. (McGraw-Hill, New York, 1990).
17. L. C. Andrews and R. L. Phillips, *Mathematical Techniques for Engineers and Scientists* (SPIE Optical Engineering Press, Bellingham, Wash., 2003).
18. W. H. Carter, "Spot size and divergence for Hermite Gaussian beams of any order," *Appl. Opt.* **19**, 1027–1029 (1980); "Energy carried over the rectangular spot within a Hermite-Gaussian beam," *Appl. Opt.* **21**, 7 (1982).
19. R. L. Phillips and L. C. Andrews, "Spot size and divergence for Laguerre Gaussian beams of any order," *Appl. Opt.* **22**, 643–644 (1983).
20. M. C. Roggeman and B. Welsh, *Imaging through Turbulence* (CRC Press, Boca Raton, 1996).